Table 4

Univariate and Multivariate Analysis of Clinical Parameters for Predicting HVPG Greater Than 10 mm Hg in the Training Set

	Univariate Analysis		Multivariate Analysis	
Parameter*	*P* Value	Odds Ratio	*P* Value	Odds Ratio
Sex	.515	0.836		
Age	.391	0.975		
Hepatic elasticity	.0001	5.901	.188	8.143
RHA/RPV ratio	.011	2.323	.869	0.901
Splenic elasticity	<.0001	6.869	.020	9.070
Spleen volume	.009	1.004	.973	1.000
AST level	.966	1.003		
ALT level	.987	1.000		
Platelet count	.005	0.738	.872	0.973
γ-GTP level	.621	1.001		
Albumin level	.003	0.252	.640	0.23
Prothrombin time	.006	0.933	.561	0.92
HOMA-IR	.126	1.143		
AST/ALT	.552	1.354		
APRI	.089	3.114		
FIB-4 index	.106	1.188		
Child-Pugh class	.178	0.987		
PI of splenic artery	.678	1.349		

* GTP = guanosine triphosphate, HOMA-IR = homeostasis model assessment of insulin resistance, PI = pulsatility index.

Table 5

Univariate and Multivariate Analysis of Clinical Parameters for Predicting HVPG Greater Than 12 mm Hg in the Training Set

	Univariate Analysis		Multivariate Analysis	
Parameter*	*P* Value	Odds Ratio	*P* Value	Odds Ratio
Sex	.529	0.831		
Age	.576	0.982		
Hepatic elasticity	.007	5.929	.354	6.171
RHA/RPV ratio	.045	1.934	.938	0.946
Splenic elasticity	.007	12.935	.040	17.708
Spleen volume	.154	1.002		
AST level	.302	1.007		
ALT level	.889	0.998		
Platelet count	.019	0.734		
γ-GTP level	.323	0.995		
Albumin level	.001	0.116		
Prothrombin time	.002	0.923		
HOMA-IR	.926	1.008		
AST/ALT	.239	1.935		
APRI	.023	4.284	.117	3.525
FIB-4 index	.009	1.221	.159	0.627
Child-Pugh class	.001	6.554	.594	1.768
PI of splenic artery	.823	0.852		

* GTP = guanosine triphosphate, HOMA-IR = homeostasis model assessment of insulin resistance, PI = pulsatility index.

elasticity is usually measured from the right lobe. Merriman et al (27) found that histologic findings frequently differed between the left and right lobes of patients with nonalcoholic fatty liver disease. This variability would induce a more distant relationship between hepatic elasticity and HVPG. Conversely, the spleen is more homogeneous than the liver and is less anatomically divided.

To our knowledge, this is the first study to measure splenic elasticity with US-based RTE. Splenic elasticity could also be noninvasively measured with MR elastography or transient elastography (FibroScan; Echosens, Paris, France). Measurements of spleen stiffness are not comparable among quantitative transient elastography, MR elastography, and qualitative RTE. However, RTE is easier, more economical, and faster and does not require a dedicated system. A trial of MR elastography (8) has revealed a close correlation between splenic and hepatic elasticity. However, the correlation between splenic elasticity and portal venous pressure measured with HVPG has not, to our knowledge, been investigated. Specific facilities are required for MR elastography, which takes more time. Thus, RTE is more practical than MR elastography in the identification of splenic elasticity.

From the practical aspects of obtaining US information about the spleen, we believe that measuring splenic elasticity with transient elastography might be very difficult because images are not visible during measurements. Thus, the images obtained with transient elastography are not seen in real time. Further studies should compare the accuracy of splenic elasticity measured with RTE to that measured with other modalities. Because we previously found that the elasticity of small vessels is suitable as a reference, we used that of the small hepatic and splenic veins as reference values in the present study (16). Moreover, such elasticity does not change over time and it does not undergo transformation with disease (eg, arteriosclerosis) (16).

Hepatic and splenic blood flow should reflect portal hypertension, and both have been assessed by using duplex

Table 6

Sensitivity, Specificity, PPV, NPV, and Diagnostic Accuracy of Cutoff Values for Splenic Elasticity in Predicting the Presence of Gastroesophageal Varices

Patient Group and Cutoff Value	Sensitivity (%)	Specificity (%)	PPV (%)	NPV (%)	Diagnostic Accuracy (%)
Training set (n = 60)					
8.24	96 (25/26)	85 (29/34)	83 (25/30)	97 (29/30)	90 (54/60)
9.99	54 (14/26)	97 (33/34)	93 (14/15)	73 (33/45)	78 (47/60)
Validation set (n = 210)					
8.24	98 (46/47)	93.8 (153/163)	82 (46/56)	99.4 (153/154)	94.8 (199/210)
9.99	26 (12/47)	99.4 (162/163)	92 (12/13)	82.2 (162/197)	82.9 (174/210)

Note.—Numbers in parentheses are numbers of patients.

Doppler US (RHA/RPV ratio) (17), the congestion index (18), splenic artery velocity (28,29), and the pulsatility and resistive indexes of the splenic artery (28,29). We also measured these US factors, but they did not associate with HVPG as much as splenic elasticity determined with RTE. We postulated that duplex Doppler US would be unreliable because a shunt could decrease the resistance of splenic venous blood outflow. In fact, a large portosystemic shunt reduces portal venous pressure by changing blood flow (30). Conversely, serum markers (AST/ALT ratio [19], APRI [20], FIB-4 index [21], homeostatis model assessment of insulin resistance) of hepatic fibrosis and splenic volume (31) have all been described as predictors of portal hypertension. However, our results contradicted these findings.

Splenomegaly is caused by congestion due to portal hypertension (32). Hepatofugal and splanchnic venous blood is shunted via portosystemic collateral vessels to the systemic circulation during severe portal hypertension to avoid high pressure in the portal vein. We measured the volume of the spleen with CT, whereas Berzigotti et al (31) measured spleen volume with two-dimensional US. Although splenic volume was shown to correlate with an HVPG of more than 10 mm Hg at univariate analysis, we could not identify a correlation between HVPG and spleen size at multivariate analysis. This could be due to the relationship between spleen volume and splenic elasticity; however, there was no correlation between those parameters (r = 0.229).

We validated that splenic elasticity measured with RTE could be a good predictor of gastroesophageal varix. The 2005 Baveno Consensus Workshop (33) and the American Association for the Study of Liver Diseases 2007 Single Topic Symposium on Portal Hypertension (34) have both recommended endoscopic screening for esophageal varices, regardless of Child-Pugh class and cause. Patients with cirrhosis and gastroesophageal varices have an HVPG of at least 10–12 mm Hg. Moreover, variceal hemorrhage does not occur when the HVPG is reduced to 12 mm Hg. Thus, we investigated 10 and 12 mm Hg as HVPG cutoffs. Our results indicated that we could estimate the presence of gastroesophageal varices from splenic elasticity. This means that we could reduce the frequency of screening-detected gastroesophageal varices by using gastrointestinal endoscopy. Otherwise, high splenic elasticity would alert operators to the need for gastrointestinal endoscopy. Splenic elasticity could be a useful clinical marker with which to estimate the prognosis of such patients. This requires evaluation in a long-term follow-up study of patients with chronic liver damage.

This study has several limitations. We did not estimate inter- and intraobserver variability when measuring splenic elasticity. Moreover, we did not directly compare splenic and hepatic elasticity. We excluded extremely obese patients because we previously showed that elasticity measured with RTE is accurate up to a body mass index of 25 (moderately obese) (16). Moreover, splenic elasticity measured with RTE would be influenced by vascular abnormalities such as collateral vessels and shunts. Further study is needed to resolve these limitations, and MR elastography might be considered for extremely obese patients.

In conclusion, splenic elasticity measured with noninvasive RTE showed close correlation with HVPG. Splenic elasticity is a useful predictive marker of gastroesophageal varix and has the potential to serve as a marker with which to estimate the prognosis of patients with chronic liver diseases.

Acknowledgments: We thank Teruhito Mochizuki, MD, PhD, Takaharu Tsuda, MD, PhD, Hiroaki Tanaka, MD, and Kenji Tanimoto for valuable contributions to this study.

Disclosures of Potential Conflicts of Interest: **M.H.** No potential conflicts of interest to disclose. **H.O.** No potential conflicts of interest to disclose. **Y. Koizumi** No potential conflicts of interest to disclose. **Y. Kisaka** No potential conflicts of interest to disclose. **M.A.** No potential conflicts of interest to disclose. **Y.I.** No potential conflicts of interest to disclose. **B.M.** No potential conflicts of interest to disclose. **Y.H.** No potential conflicts of interest to disclose. **M.O.** No potential conflicts of interest to disclose.

References

1. Mahl TC, Groszmann RJ. Pathophysiology of portal hypertension and variceal bleeding. Surg Clin North Am 1990;70(2):251–266.
2. D'Amico G, Garcia-Tsao G, Pagliaro L. Natural history and prognostic indicators of survival in cirrhosis: a systematic review of 118 studies. J Hepatol 2006;44(1):217–231.
3. Salerno F, Guevara M, Bernardi M, et al. Refractory ascites: pathogenesis, definition and therapy of a severe complication in patients with cirrhosis. Liver Int 2010;30(7):937–947.
4. Lee JM, Han KH, Ahn SH. Ascites and spontaneous bacterial peritonitis: an Asian perspective. J Gastroenterol Hepatol 2009;24(9):1494–1503.
5. Thalheimer U, Leandro G, Samonakis DN, Triantos CK, Patch D, Burroughs AK. Assessment of the agreement between wedge hepatic vein pressure and portal vein pressure in cirrhotic patients. Dig Liver Dis 2005;37(8):601–608.

6. Ripoll C, Bañares R, Rincón D, et al. Influence of hepatic venous pressure gradient on the prediction of survival of patients with cirrhosis in the MELD era. Hepatology 2005; 42(4):793–801.

7. D'Amico G, Garcia-Pagan JC, Luca A, Bosch J. Hepatic vein pressure gradient reduction and prevention of variceal bleeding in cirrhosis: a systematic review. Gastroenterology 2006;131(5):1611–1624.

8. Talwalkar JA, Yin M, Venkatesh S, et al. Feasibility of in vivo MR elastographic splenic stiffness measurements in the assessment of portal hypertension. AJR Am J Roentgenol 2009;193(1):122–127.

9. Manenti A, Botticelli A, Gibertini G, Botticelli L. Experimental congestive splenomegaly: histological observations in the rat. Pathologica 1993;85(1100):721–724.

10. Cavalli G, Re G, Casali AM. Red pulp arterial terminals in congestive splenomegaly: a morphometric study. Pathol Res Pract 1984;178(6):590–594.

11. Re G, Casali AM, Cavalli D, Guida G, Cau R, Cavalli G. Histometric analysis of white pulp arterial vessels in congestive splenomegaly. Appl Pathol 1986;4(1-2):98–103.

12. Terayama N, Makimoto KP, Kobayashi S, et al. Pathology of the spleen in primary biliary cirrhosis: an autopsy study. Pathol Int 1994;44(10-11):753–758.

13. Vizzutti F, Arena U, Rega L, et al. Performance of Doppler ultrasound in the prediction of severe portal hypertension in hepatitis C virus–related chronic liver disease. Liver Int 2007;27(10):1379–1388.

14. Vizzutti F, Arena U, Romanelli RG, et al. Liver stiffness measurement predicts severe portal hypertension in patients with HCV-related cirrhosis. Hepatology 2007;45(5):1290–1297.

15. Carrión JA, Navasa M, Bosch J, Bruguera M, Gilabert R, Forns X. Transient elastography for diagnosis of advanced fibrosis and portal hypertension in patients with hepatitis C recurrence after liver transplantation. Liver Transpl 2006;12(12):1791–1798.

16. Koizumi Y, Hirooka M, Kisaka Y, et al. Liver fibrosis in patients with chronic hepatitis C: noninvasive diagnosis by means of real-time tissue elastography: establishment of the method for measurement. Radiology 2011; 258(2):610–617.

17. Hirata M, Akbar SM, Horiike N, Onji M. Noninvasive diagnosis of the degree of hepatic fibrosis using ultrasonography in patients with chronic liver disease due to hepatitis C virus. Eur J Clin Invest 2001;31(6):528–535.

18. Moriyasu F, Nishida O, Ban N, et al. "Congestion index" of the portal vein. AJR Am J Roentgenol 1986;146(4):735–739.

19. Sheth SG, Flamm SL, Gordon FD, Chopra S. AST/ALT ratio predicts cirrhosis in patients with chronic hepatitis C virus infection. Am J Gastroenterol 1998;93(1):44–48.

20. Wai CT, Greenson JK, Fontana RJ, et al. A simple noninvasive index can predict both significant fibrosis and cirrhosis in patients with chronic hepatitis C. Hepatology 2003;38(2):518–526.

21. Sterling RK, Lissen E, Clumeck N, et al. Development of a simple noninvasive index to predict significant fibrosis in patients with HIV/HCV coinfection. Hepatology 2006; 43(6):1317–1325.

22. Ozaki K, Matsui O, Kobayashi S, et al. Selective atrophy of the middle hepatic venous drainage area in hepatitis C–related cirrhotic liver: morphometric study by using multidetector CT. Radiology 2010;257(3): 705–714.

23. Pinzani M, Gentilini P. Biology of hepatic stellate cells and their possible relevance in the pathogenesis of portal hypertension in cirrhosis. Semin Liver Dis 1999;19(4): 397–410.

24. Bosch J, Garcia-Pagan JC. Pathophysiology of portal hypertension and its complications. In: Bircher J, Benhamou JP, McIntyre N, Rizzetto M, Rodes J, eds. Oxford textbook of clinical hepatology. 2nd ed. Vol 1. New York, NY: Oxford University Press, 1999; 653–660.

25. Wiest R, Groszmann RJ. The paradox of nitric oxide in cirrhosis and portal hypertension: too much, not enough. Hepatology 2002;35(2):478–491.

26. Gupta TK, Toruner M, Chung MK, Groszmann RJ. Endothelial dysfunction and decreased production of nitric oxide in the intrahepatic microcirculation of cirrhotic rats. Hepatology 1998;28(4):926–931.

27. Merriman RB, Ferrell LD, Patti MG, et al. Correlation of paired liver biopsies in morbidly obese patients with suspected nonalcoholic fatty liver disease. Hepatology 2006; 44(4):874–880.

28. Bolognesi M, Sacerdoti D, Merkel C, et al. Splenic Doppler impedance indices: influence of different portal hemodynamic conditions. Hepatology 1996;23(5):1035–1040.

29. Liu CH, Hsu SJ, Liang CC, et al. Esophageal varices: noninvasive diagnosis with duplex Doppler US in patients with compensated cirrhosis. Radiology 2008;248(1):132–139.

30. Osada Y, Kanazawa H, Narahara Y, Mamiya Y, Nakatsuka K, Sakamoto C. Wedged hepatic venous pressure does not reflect portal pressure in patients with cirrhosis and hepatic veno-venous communications. Dig Dis Sci 2008;53(1):7–13.

31. Berzigotti A, Zappoli P, Magalotti D, Tiani C, Rossi V, Zoli M. Spleen enlargement on follow-up evaluation: a noninvasive predictor of complications of portal hypertension in cirrhosis. Clin Gastroenterol Hepatol 2008; 6(10):1129–1134.

32. Bolognesi M, Merkel C, Sacerdoti D, Nava V, Gatta A. Role of spleen enlargement in cirrhosis with portal hypertension. Dig Liver Dis 2002;34(2):144–150.

33. de Franchis R. Evolving consensus in portal hypertension: report of the Baveno IV consensus workshop on methodology of diagnosis and therapy in portal hypertension. J Hepatol 2005;43(1):167–176.

34. Garcia-Tsao G, Sanyal AJ, Grace ND, Carey W; Practice Guidelines Committee of the American Association for the Study of Liver Diseases; Practice Parameters Committee of the American College of Gastroenterology. Prevention and management of gastroesophageal varices and variceal hemorrhage in cirrhosis. Hepatology 2007; 46(3):922–938.

Mass Reduction by Radiofrequency Ablation Before Hepatic Arterial Infusion Chemotherapy Improved Prognosis for Patients With Huge Hepatocellular Carcinoma and Portal Vein Thrombus

Masashi Hirooka[1]
Yohei Koizumi
Yoshiyasu Kisaka
Masanori Abe
Hidehiro Murakami
Bunzo Matsuura
Yoichi Hiasa
Morikazu Onji

OBJECTIVE. The prognosis for patients with advanced large hepatocellular carcinoma (HCC) with portal vein (PV) tumor thrombosis remains poor, and treatment is usually limited to hepatic arterial infusion (HAI) chemotherapy. In this study, we first performed mass reduction using radiofrequency ablation (RFA), followed by HAI chemotherapy. Prognosis after this treatment was evaluated.

SUBJECTS AND METHODS. HCC with PV tumor thrombosis was diagnosed in 20 patients between April 2004 and December 2008, and treatment was performed using mass-reduction therapy by RFA before HAI chemotherapy. For comparison, 33 patients treated with HAI chemotherapy without RFA were retrospectively selected as historical control subjects under the same conditions. Prognosis in each group was evaluated.

RESULTS. Mass-reduction therapy by RFA combined with HAI chemotherapy achieved complete response in six patients (30%), partial response in 11 patients (55%), stable disease in two patients (10%), and progressive disease in one patient (5%). Among the control subjects, complete response was seen in 0 patients (0%), partial response in 12 patients (33.3%), stable disease in 16 patients (44.4%), and progressive disease in eight patients (22.2%). The cumulative survival rates for those who received the combined therapy at 6, 12, and 24 months were 100%, 89.7%, and 78.8%, respectively. The median survival was 953 days (95% CI, 760–1,102 days). In the control subjects, the cumulative survival rates at 6, 12, and 24 months were 84.9%, 56.1%, and 16.9%, respectively ($p < 0.0001$). No serious adverse events were encountered in either group.

CONCLUSION. For patients with huge HCC and PV tumor thrombosis, mass-reduction treatment by RFA before HAI chemotherapy is safe and can improve prognosis.

Keywords: hepatic arterial infusion chemotherapy, hepatocellular carcinoma, portal vein tumor thrombosis, radiofrequency ablation

DOI:10.2214/AJR.09.2852

Received April 4, 2009; accepted after revision July 22, 2009.

[1]All authors: Department of Gastroenterology and Metabology, Ehime University Graduate School of Medicine, Shizukawa 454, Toon-shi, Ehime 791-0295, Japan. Address correspondence to Yoichi Hiasa (hiasa@m.ehime-u.ac.jp).

WEB
This is a Web exclusive article.

AJR 2010; 194:W221–W226

0361–803X/10/1942–W221

The prognosis is very poor for patients with hepatocellular carcinoma (HCC) invading the major branches of the portal vein (PV). PV tumor thrombus is associated with the threat of bleeding of the esophageal varices or hepatic failure. Thus, the patient's quality of life is poor.

In several studies, investigators have reported treatment of advanced HCC with PV tumor thrombosis using conventional treatments such as hepatectomy [1, 2], transcatheter hepatic arterial embolization [3], and chemotherapy [4–7]. With regard to aggressive treatment of HCC with PV tumor thrombosis, no acceptable outcomes have yet been obtained. Hepatic arterial infusion (HAI) chemotherapy has recently been reported to improve response rate and survival [4–6]. Although HAI chemotherapy has been attempted widely, the effectiveness of HAI chemotherapy remains unsatisfactory. Studies have revealed that adjuvant HAI chemotherapy after hepatectomy for HCC with PV tumor thrombosis is very effective [1, 8]. However, hepatectomy for small HCC is considered excessively invasive. Hepatectomy for advanced HCC certainly places a considerable burden on the patient. Conversely, radiofrequency ablation (RFA) is less invasive than hepatectomy. With developments in technique for RFA, large HCC and PV tumor thrombosis also can be treated by RFA [9–12].

We therefore propose a new method for the treatment of advanced HCC—using RFA for mass reduction of the tumor before HAI chemotherapy. The aim of this study was to evaluate the safety of this method and the prognosis of patients treated with this method compared with patients who had undergone conventional HAI chemotherapy without RFA.

Subjects and Methods

Patients and Inclusion Criteria

Twenty patients (16 men, four women; mean age, 63.9 ± 7.7 [SD] years) who had been admitted to the Department of Gastroenterology and Metabology of the Ehime University Hospital in Japan between April 2004 and December 2008 were diagnosed with HCC with PV tumor thrombosis. After we had obtained written, informed consent from study participants, mass-reduction therapy by RFA was performed before HAI chemotherapy. This prospective cohort study was conducted in accordance with the Declaration of Helsinki.

The criteria for study inclusion were as follows: first, Eastern Cooperative Oncology Group (ECOG) performance status of 0–2; second, successful implantation of an intraarterial catheter and drug delivery system; third, the existence of a giant nodule < 15 cm in diameter or of spread of tumor to comprise < 50% of the total liver volume; fourth, platelet count of > 70,000/mm^3; fifth, granulocyte count of > 2,500/mm^3; sixth, creatinine clearance of > 60 mL/h; and, seventh, the absence of extrahepatic metastasis. HCC was diagnosed on the basis of histologic findings; imaging studies; and elevated serum α-fetoprotein level, des-γ-carboxy prothrombin (DCP) level, or both.

Thirty-three patients (30 men, three women; mean age, 62.4 ± 7.8 [SD] years) had been treated using HAI chemotherapy without mass-reduction therapy by RFA between January 2002 and December 2008, and these patients were used as historical control subjects. Informed consent was obtained from all prospective subjects before they participated in the trial but was not obtained for retrospective data from historical control subjects. This study was approved by the ethics committee at Ehime University Hospital.

Catheter Implantation

Celiac angiography was performed using the femoral approach with the patient under local anesthesia. A 5-French heparin-coated catheter was introduced into the proper or common hepatic artery. The gastroduodenal artery and right gastric artery were occluded with steel coils to prevent gastroduodenal injury from anticancer agents. Aberrant hepatic arteries, if present, were occluded with metallic coils or a 1:1.5 mixture of *N*-butyl cyanoacrylate and iodized oil before treatment of hepatic arterial redistribution [13]. After the catheter was connected to the injection port, the device was implanted in a subcutaneous pocket in a femoral site. Patients received regional chemotherapy via the hepatic artery through a subcutaneously implanted port.

Treatment Protocol for Chemotherapy

We started the chemotherapy after the patients' complications (i.e., fever, elevation of transaminase level) from RFA had improved. Each patient received subcutaneous pegylated interferon (Peg-Intron, Schering-Plough Pharmaceuticals) and intraarterial infusion of 5-fluorouracil (5-FU Injection 250, Kyowa Hakko). One cycle of treatment lasted 4 weeks. Pegylated interferon (50 μg) was administered subcutaneously on days 1, 8, 15, and 22. Continuous infusion chemotherapy (300 mg/m^2/d of 5-fluorouracil) through the proper hepatic artery was administered in weeks 1 and 2 using the implanted drug-delivery system. A 2- or 3-week rest period separated each treatment cycle. All anticancer therapies were discontinued when adverse events reached level 2 according to ECOG classifications. At least two cycles of chemotherapy were performed.

Mass Reduction by RFA

Before mass-reduction treatment was performed, 15 mg of pentazocine hydrochloride and 25 mg of hydroxyzine hydrochloride were administered intramuscularly. Local anesthesia was induced using 5 mL of 1% lidocaine hydrochloride injected through the skin into the peritoneum along a predetermined puncture line. The radiologist performing the procedure inserted a 20-cm-long 17-gauge radiofrequency electrode equipped with a 2- or 3-cm-long exposed metallic tip (Cool-tip, Valleylab) or expandable needle (LeVeen Needle, Boston Scientific). If the diameter of the tumor was more than 5 cm, a 4-cm expandable needle was selected. The Cool-tip needle was used for the PV tumor thrombosis, in which the tumor had a diameter of less than 5 cm. This single needle also was used for residual lesion after ablating by LeVeen needle according to the protocol noted above. If the lung was obstructing the view of the nodule, 500 mL of saline was injected into the right pleural cavity [14].

Ablation was first performed for the intraparenchymal nodule, then the PV tumor thrombosis was treated. During the treatment of PV tumor thrombosis, RFA was performed first for the main portal branch, followed by ablation for PV tumor thrombosis in the peripheral branches. The electrode needle was inserted into the portal thrombus as close to the major axis of the PV tumor thrombosis as possible. A single needle was used to prevent injury to the major branches of the bile duct or artery. The electrode output was set as low as possible (i.e., < 50 W). If the hyperechoic area was not covered for the PV tumor thrombosis, an ethanol injection was added. Ethanol was injected until hyperechoic change of the target area could be seen. Usually, we injected 4 mL or less of ethanol for each session.

After the treatment, we evaluated the efficacy of RFA using CT. Complete necrosis was achieved for all ablated nodules except nonablated daughter nodules. We decided to perform the additional treatment if the viable portion remained by the time of the CT evaluation.

Estimation of Therapeutic Effect

Posttreatment evaluation was performed every 3 months. The evaluation mainly comprised periodic sonography; CT; and tests for tumor markers, including α-fetoprotein and DCP, for all patients. Objective response was classified according to ECOG criteria [15].

Statistical Analysis

Data are expressed as means ± SD. Statistical analysis was performed using the Student's *t* test for unpaired data, contingency table analysis, and the Mann-Whitney *U* test as appropriate. Cumulative survival curves were constructed using the Kaplan-Meier method. Values of $p < 0.05$ were considered to represent statistical significance.

Results

The Estimation of RFA

Only the Cool-tip needle was used for 20 cases, and both the Cool-tip needle and LeVeen needle were used for 14 cases. In no case was only the LeVeen needle used. Except tumor diameter, there was no significant difference between the cases treated using only the Cool-tip needle (47.4 ± 14.2 mm) and the cases treated using two needles (65.9 ± 22.1 mm) (p = 0.117). Ethanol injection was performed for four patients. The median volume of ethanol was 3.8 ± 0.3 mL (range, 3.5–4.2 mL). The mean number of RFA electrode punctures in each session was 3.0 ± 1.1 (range, 2–7). We ablated the small daughter nodules if there were two or more.

Post-RFA Complications

The mean number of ablation sessions was 1.7 ± 0.7 (range, 1–3). Complete necrosis of the PV thrombosis was achieved in 17 patients (85%). No serious adverse events were observed after ablation. No patients displayed liver abscess or bleeding, but all patients showed a transient elevation of aspartate aminotransferase (AST) and alanine aminotransferase (ALT). The maximum values of AST and ALT after mass reduction by RFA were 221 and 251 IU/L, respectively. Elevation of ALT was mild (< 150 IU/L) in 10 patients and moderate (150–600 IU / L) in 10 patients. None of the patients showed severe ALT elevation (> 600 IU/L). The ALT level for all patients had recovered within 1 month after RFA. The median interval between the final

ablation until the start of chemotherapy was 9.1 ± 2.8 days (range, 5–14 days).

Clinical Response to Combination Therapy

Table 1 summarizes the characteristics of all the patients and control subjects. All patients completed at least two cycles of chemotherapy after RFA. For patients who displayed a clinical response, we continued chemotherapy until HCC progressed. If complete response was achieved, chemotherapy was stopped after the second cycle. Treatment was stopped after completion of the second cycle in patients with no response because of extended progression of HCC. The mean number of treatment cycles was 3.4 ± 2.2 (range, 2–10).

Among the 20 patients treated with RFA before HAI chemotherapy, six patients (30%) showed complete response; 11 (55%), partial response; two (10%), stable disease; and one (5%), progressive disease. In comparison, the control group showed complete response in 0 patients (0%), partial response in 12 (33.3%), stable disease in 16 (44.4%), and progressive disease in eight (22.2%) (Table 2). Of the 20 patients, six patients had PV tumor thrombosis in the main portal trunk and 14 in the major portal branch (Table 1). The response rate in these six patients who had PV tumor thrombosis in the major portal trunk was not significantly worse (83.3%) than that in the other 14 patients (response rate, 92.8%) ($p = 0.199$).

The response rate was significantly better for the mass-reduction group than for the control subjects ($p < 0.0001$). In four patients (20%), patency of the PV was achieved after combination treatment; in eight patients, partial PV patency was seen. Although the viable lesion in the PV tumor thrombosis had disappeared after treatment in two patients, PV flow did not resume in either patient, and cavernous transformation occurred. In the control group, complete patency of the PV occurred for 0 patients and partial patency, for seven patients. The repatency rate of the PV was significantly better ($p = 0.0016$) in the mass-reduction group than in the control group.

In the mass-reduction group, intrahepatic recurrence after chemotherapy was seen in three patients and extrahepatic recurrence, in five patients. In the control group, intrahepatic and extrahepatic recurrence was noted in eight and three patients, respectively ($p = 0.1016$). In the mass-reduction group, the cumulative survival rates at 6, 12, and 24 months were 100%, 89.7%, and 78.8%, respectively. The median survival time was 953 days (95% CI, 760–1,102 days). In the control group, the cumulative survival rates at 6, 12, and 24 months were 84.9%, 56.1%, and 16.9%, respectively. The median survival time was 352 days (95% CI, 267–407 days).

TABLE 1: Patient and Tumor Characteristics

Characteristic	Patients Who Received HAI Chemotherapy After RFA ($n = 20$)	Historical Control Subjects ($n = 33$)	p
Sex (no. of patients)			0.26
Male	16	30	
Female	4	3	
Age (y)			0.49
Mean ± SD	63.9 ± 7.7	62.4 ± 7.8	
Cause			0.76
Hepatitis B virus	5	6	
Hepatitis C virus	14	26	
Other[a]	1	1	
Child-Pugh class			0.72
A	16	25	
B	4	8	
Tumor diameter (mm)			0.40
Mean ± SD	57.3 ± 20.9	59.1 ± 28.5	
Extent of PV tumor thrombosis			0.26
Main portal trunk	6	15	
Major portal branch	14	18	

Note—HAI = hepatic arterial infusion, RFA = radiofrequency ablation, PV = portal vein.
[a]Non–hepatitis B virus, non–hepatitis C virus.

Overall survival rates were significantly improved for the mass-reduction group compared with control subjects ($p < 0.0001$, Fig. 1). The causes of death were as follows in the mass-reduction group: extension of cancer, nine patients; hepatic failure, none; gastroesophageal bleeding, two patients; and other cause, one patient. In the control group, the causes of death were extension of cancer, 27 patients; hepatic failure, two; gastroesophageal bleeding, one patient; and other cause, one patient ($p = 0.573$). Patients and control subjects died and tumor recurrences were noted during both periods of HAI chemotherapy and after cessation of HAI chemotherapy. The frequency between them was not different statistically.

Case Presentation

A 55-year-old man underwent RFA for HCC in January 2006. The largest HCC nodule (6.5 × 6.0 cm) in the right lobe was ablated using a 4.5-cm expandable needle. After mass reduction of the intrahepatic lesion, PV tumor thrombosis in the main and right portal branches was ablated using a single RFA needle. HAI chemotherapy (two cycles) was performed 11 days after the reduction therapy,

TABLE 2: Response to Hepatic Arterial Infusion (HAI) Chemotherapy in Patients Who Underwent Radiofrequency Ablation (RFA) and in Control Subjects Who Did Not

Response	Patients Who Received HAI Chemotherapy After RFA ($n = 20$)	Historical Control Subjects ($n = 36$)
Complete response	6	0
Partial response	11	12
Stable disease	2	16
Progressive disease	1	8
Response rate (%)	85.0	33.3
p	< 0.0001	

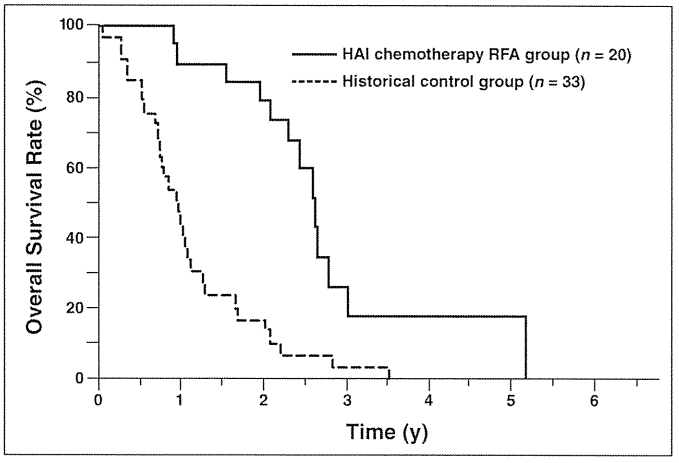

Fig. 1—Graph shows cumulative overall survival rates after hepatic arterial infusion (HAI) chemotherapy with and without radiofrequency ablation (RFA). Survival rate was higher for patients who underwent HAI chemotherapy and RFA than for control subjects who underwent HAI chemotherapy only ($p < 0.0001$).

and subsequent CT showed complete necrosis of tumor thrombosis. All tumor marker levels, which had been abnormal before treatment, normalized after RFA and HAI chemotherapy: α-fetoprotein level, from 580.4 to 2.5 ng/mL; α-fetoprotein-L3, from 43.1% to 0%; and DCP, from 598 to 27 mAU/mL (Fig. 2). This patient has undergone follow-up on an outpatient basis, with no evidence of recurrence as of the time of writing.

Discussion

The prognosis for patients with advanced HCC with PV tumor thrombosis remains poor [16]. The median survival time of HCC patients with PV tumor thrombosis is reportedly approximately 90 days with supportive care [17]. Many therapeutic modalities have been proposed to improve survival rate [1–8], but no standard treatment protocol has yet been defined.

HAI chemotherapy using implanted reservoirs has achieved significant survival benefits for patients with advanced HCC. Ishida et al. [4] reported that HAI chemotherapy with degradable starch microspheres (Spherex, Yakult) achieved an 84.6% response rate, with 1-, 2-, and 3-year survival rates of 100%, 28.9%, and 9.6%, respectively, in all patients and 100%, 33.3%, and 0% in patients with PV tumor thrombosis. The median survival was 22.1 months in all patients and 17.1 months in the six patients with PV tumor thrombosis [4].

If patients have a huge HCC mass with PV tumor thrombosis, response to treatment and survival are worsened [5]. Antitumor effects of those treatments against a huge mass of HCC are considered to be reduced for the following reasons: First, as HCC grows from the moderately differentiated type to the poorly or undifferentiated type, hypovascular changes occur, reducing the ability of anticancer drugs to be delivered to the advanced HCC. Second, huge HCC tumors are often located on the hepatic surface and are often fed by extrahepatic arteries, such as the adrenal or intercostal arteries [18, 19]. Again, this serves to reduce delivery of the anticancer drug from the hepatic artery. Third, in patients with huge HCC, particularly those with PV tumor thrombosis, portal flow is stagnated by invasion of the HCC, reducing liver function [16]. Moreover, delivery of anticancer drugs is again reduced in such cases. Given these factors, assistance by mass-reduction treatment seemed likely to prove useful for patients with huge HCC with PV tumor thrombosis and could improve prognosis compared with HAI chemotherapy monotherapy.

Mass-reduction therapy for patients with huge HCC nodules and PV tumor thrombosis could be compared with transcatheter arterial embolization (TAE) or surgical resection. TAE is a useful method for treating huge nodules. However, TAE requires injection of embolization material through a catheter into the hepatic artery. The response of huge HCC to TAE is often insufficient because of the reasons mentioned earlier. Moreover, if cavernous transformation of the PV has not occurred in cases of HCC with PV tumor thrombosis, parenchymal infarction around HCC can result from TAE, further damaging the liver. TAE is unsuitable for mass-reduction treatment of huge HCC.

Recently, the results of ^{90}Y therapy for huge HCC have been reported [20]. In Japan, we cannot use ^{90}Y therapy. Because ^{90}Y therapy is radiochemoembolization, ^{90}Y therapy is not suitable for treatment of recurrences. Riaz et al. [20] reported that the rate of complete necrosis by the treatment of ^{90}Y was only 17% of the tumor for tumors more than 5 cm in diameter, whereas complete necrosis was achieved in all nodules more than 5 cm using our RFA method.

The most curative approach to treating huge HCC with PV tumor thrombosis is surgical resection. However, this option is feasible in only a minority of HCC patients because most patients with huge HCC with PV tumor thrombosis display seriously compromised liver function. Abdominal open surgery is thus too invasive for patients with a limited prognosis. Local ablation therapy for huge HCC has recently been reported [9, 10]. Wider lesions of the liver can be ablated using a multipolar needle and large expandable needle.

For the current study, we performed mass-reduction treatment using RFA and tried to treat PV tumor thrombosis aggressively. In our study, four patients with Child-Pugh grade B cirrhosis showed no deterioration of liver function after ablation of wide HCC lesions. Livraghi et al. [21] reported their first experience of treating PV tumor thrombosis using percutaneous ethanol injection (PEI). Conversely, Giorgio et al. [11] reported treatment of PV tumor thrombosis using RFA.

For the treatment of PV tumor thrombosis, RFA seems more risky than PEI. The risk of bleeding is thought to be higher because the RFA needle that is inserted into the PV is thicker than the PEI needle. Moreover, PVs accompany bile ducts and the hepatic arteries in the liver. If bile ducts and hepatic arteries are injured by RFA for PV tumor thrombosis, severe complications such as biloma, obstructive jaundice, liver abscess, and mass liver infarction can result. We performed RFA for PV tumor thrombosis with a low output (< 50 W), and none of these complications occurred in any of the patients in our study group.

Giorgio et al. [11] reported 10 cases of advanced HCC with PV tumor thrombosis treated using RFA (mean tumor diameter, 4.20 ±

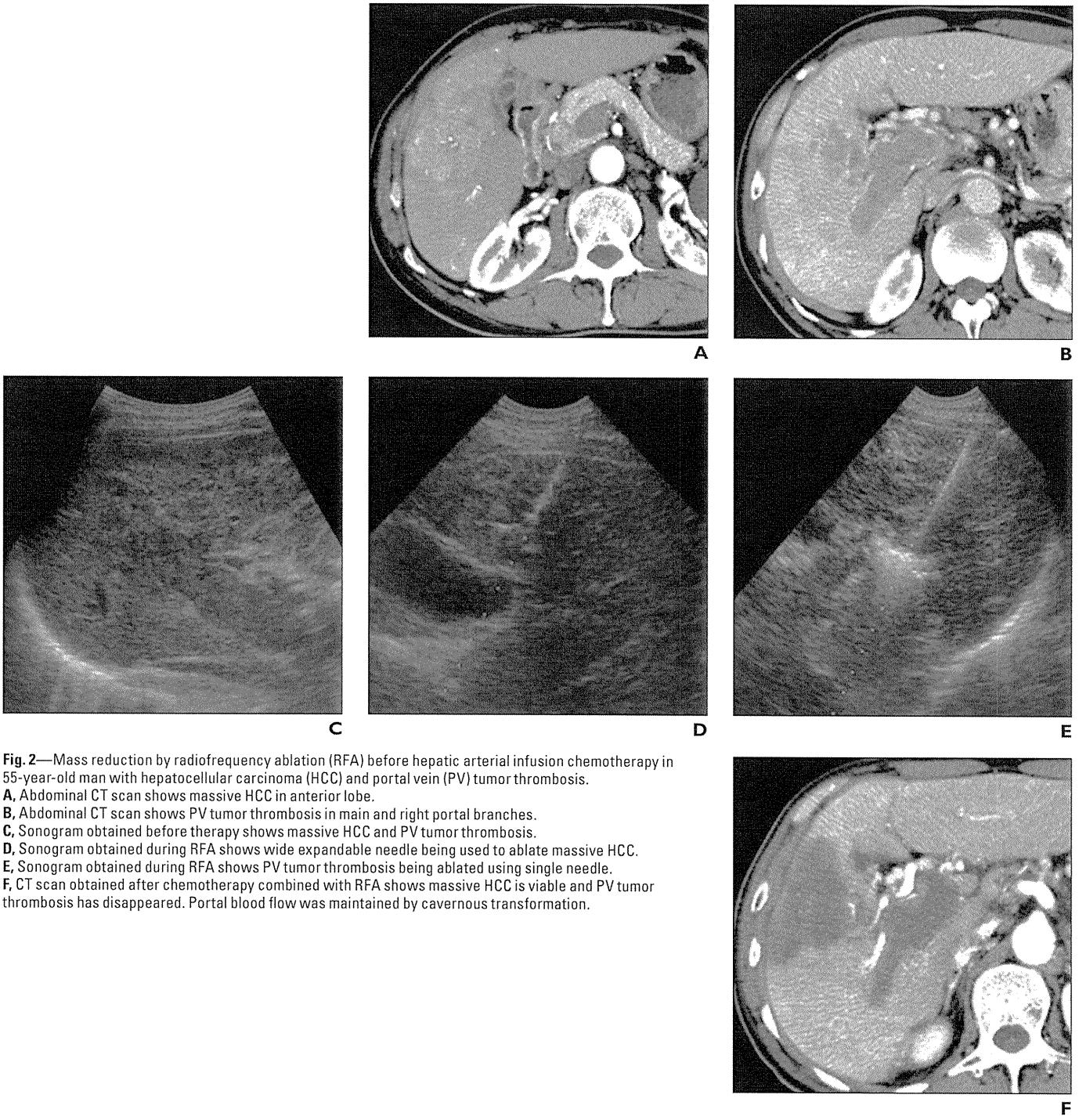

Fig. 2—Mass reduction by radiofrequency ablation (RFA) before hepatic arterial infusion chemotherapy in 55-year-old man with hepatocellular carcinoma (HCC) and portal vein (PV) tumor thrombosis.
A, Abdominal CT scan shows massive HCC in anterior lobe.
B, Abdominal CT scan shows PV tumor thrombosis in main and right portal branches.
C, Sonogram obtained before therapy shows massive HCC and PV tumor thrombosis.
D, Sonogram obtained during RFA shows wide expandable needle being used to ablate massive HCC.
E, Sonogram obtained during RFA shows PV tumor thrombosis being ablated using single needle.
F, CT scan obtained after chemotherapy combined with RFA shows massive HCC is viable and PV tumor thrombosis has disappeared. Portal blood flow was maintained by cavernous transformation.

0.36 cm; range, 3.8–4.9 cm). Although the grade of HCC was more serious in our study, our results in terms of survival time (6-, 12-, and 24-month rates of 100%, 89.7%, and 78.8%, respectively) were also good. In four cases in which ablation by RFA was insufficient, we performed PEI for the treatment of PV tumor thrombosis. In all four patients, complete PV flow resumed (Fig. 3).

In some patients, the RFA needle may not reach the far side of the liver where PV tumor thrombosis has expanded to the superior mesenteric vein or splenic vein. Fortunately, we did not encounter any such cases in this study. However, radiotherapy should be considered in such cases.

The effects of radiation associated with mass-reduction treatment and HAI chemotherapy need to be evaluated in a future study. More or less arterial–portal shunting was noted by angiography in all patients who had the PV tumor thrombosis. Our results of the treatment in the patients who had arterial–portal shunting was not bad, indicating that the arterial–portal shunting might not induce the attenuation of the effect of chemotherapy.

In conclusion, we propose a less invasive combined technique using mass-reduction

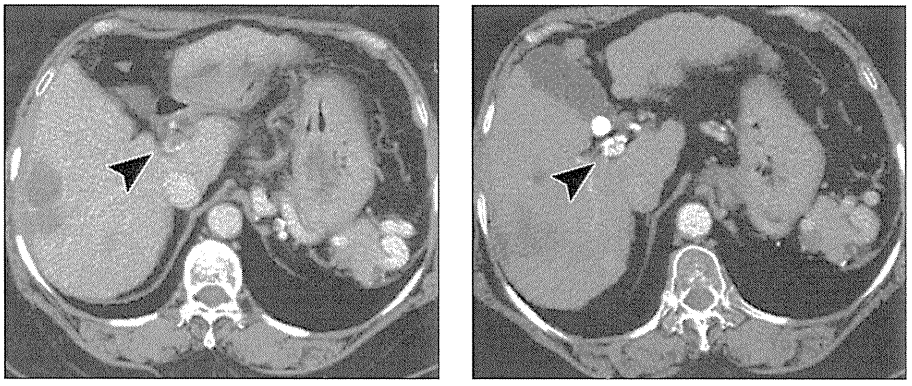

Fig. 3—Improvement of portal blood flow in 72-year-old woman with portal vein (PV) tumor thrombosis who underwent hepatic arterial infusion chemotherapy after radiofrequency ablation.
A, CT scan obtained before patient underwent combined therapy shows lumen of portal major trunk is occluded by PV tumor thrombosis (*arrowhead*).
B, CT scan obtained after patient received combined therapy shows blood flow of portal major trunk (*arrowhead*) has recovered.

treatment by RFA and HAI chemotherapy for the treatment of huge HCC and PV tumor thrombosis. This treatment appears safe and beneficial for patients showing huge HCC with PV tumor thrombosis, improving prognosis.

References

1. Fukuda S, Okuda K, Imamura M, Imamura I, Eriguchi N, Aoyagi S. Surgical resection combined with chemotherapy for advanced hepatocellular carcinoma with tumor thrombus: report of 19 cases. *Surgery* 2002; 131:300–310
2. Inoue Y, Hasegawa K, Ishizawa T, et al. Is there any difference in survival according to the portal tumor thrombectomy method in patients with hepatocellular carcinoma? *Surgery* 2009; 145:9–19
3. Chung JW, Park JH, Han JK, Choi BI, Han MC. Hepatocellular carcinoma and portal vein invasion: result of treatment with transcatheter oily chemoembolization. *AJR* 1995; 165:315–321
4. Ishida K, Hirooka M, Hiraoka A, et al. Treatment of hepatocellular carcinoma using arterial chemoembolization with degradable starch microspheres and continuous arterial infusion of 5-fluorouracil. *Jpn J Clin Oncol* 2008; 38:596–603
5. Sakon M, Nagano H, Dono K, et al. Combined intraarterial 5-fluorouracil and subcutaneous interferon-alpha therapy for advanced hepatocellular carcinoma with tumor thrombi in the major portal branches. *Cancer* 2002; 94:435–442
6. Obi S, Yoshida H, Toune R, et al. Combination therapy of intra-arterial 5-fluorouracil and systemic interferon alpha for advanced hepatocellular carcinoma with portal venous invasion. *Cancer* 2006; 106:1990–1997
7. Ando E, Yamashita F, Tanaka M, et al. A novel chemotherapy for advanced hepatocellular carcinoma with tumor thrombosis of the main trunk of the portal vein. *Cancer* 1997; 79:1890–1896
8. Nagano H, Miyamoto A, Wada H, et al. Interferon alpha and 5-fluorouracil combination therapy after palliative hepatic resection in patients with advanced hepatocellular carcinoma, portal venous tumor thrombus in the major trunk, and multiple nodules. *Cancer* 2007; 110:2493–2501
9. Takaki H, Yamakado K, Uraki J, et al. Radiofrequency ablation combined with chemoembolization for the treatment of hepatocellular carcinomas larger than 5 cm. *J Vasc Interv Radiol* 2009; 20:217–224
10. Chen MH, Yang W, Zou MW, Solbiati L, Liu JB, Dai Y. Large liver tumors: protocol for radiofrequency ablation and its clinical application in 110 patients—mathematic model, overlapping mode, and electrode placement process. *Radiology* 2004; 232:260–271
11. Giorgio A, Stefano G, Sarno A, et al. Radiofrequency ablation of hepatocellular carcinoma extended into the portal vein: preliminary results. *J Ultrasound* (in press)
12. Zheng RQ, Kudo M, Minami Y, Inui K, Chung H. Stage IV hepatocellular carcinoma with portal venous tumor thrombus: complete response after combined therapy of repeated arterial chemoembolization and radiofrequency ablation. *J Gastroenterol* 2003; 38:406–409
13. Stoesslein F, Ditscherlein G, Romaniuk PA. Experimental studies on new liquid embolization mixtures (Histoacryl-Lipiodol, Histoacryl-Pantopaque). *Cardiovasc Intervent Radiol* 1982; 5: 264–267
14. Uehara T, Hirooka M, Ishida K, et al. Percutaneous ultrasound-guided radiofrequency ablation of hepatocellular carcinoma used with artificially-induced pleural effusion and ascites. *J Gastroenterol* 2007; 42:306–311
15. Oken MM, Creech RH, Tormey DC, et al. Toxicity and response criteria of the Eastern Cooperative Oncology Group. *Am J Clin Oncol* 1982; 5: 649–655
16. Kudo M, Chung H, Haji S, et al. Validation of a new prognostic staging system for hepatocellular carcinoma: the JIS score compared with the CLIP score. *Hepatology* 2004; 40:1396–1405
17. Takizawa D, Kakizaki S, Sohara N, et al. Hepatocellular carcinoma with portal vein tumor thrombosis: clinical characteristics, prognosis, and patient survival analysis. *Dig Dis Sci* 2007; 52:3290–3295
18. Miyama S, Matsui O, Taki K, et al. Extrahepatic blood supply to hepatocellular carcinoma: angiographic demonstration and transcatheter arterial chemoembolization. *Cardiovasc Intervent Radiol* 2006; 29:39–48
19. Park SI, Lee DY, Won JY, Lee JT. Extrahepatic collateral supply of hepatocellular carcinoma by the intercostal artery. *J Vasc Interv Radiol* 2003; 14:461–468
20. Riaz A, Kulik L, Lewandowski RJ, et al. Radiologic–pathologic correlation of hepatocellular carcinoma treated with internal radiation using yttrium-90 microspheres. *Hepatology* 2009; 49: 1185–1193
21. Livraghi T, Grigioni W, Mazziotti A, Sangalli G, Vettori C. Percutaneous alcohol injection of portal thrombosis in hepatocellular carcinoma: a new possible treatment. *Tumori* 1990; 76:394–397

Liver INTERNATIONAL
OFFICIAL JOURNAL OF THE INTERNATIONAL ASSOCIATION FOR THE STUDY OF THE LIVER

Liver International ISSN 1478-3223

BASIC STUDIES

Regulatory natural killer cells in murine liver and their immunosuppressive capacity

Osamu Yoshida[1], Sheikh Mohammad Fazle Akbar[1,2], Shiyi Chen[1], Teruki Miyake[1], Masanori Abe[1], Hidetaka Murakami[1], Yoichi Hiasa[1] and Morikazu Onji[1]

1 Department of Gastroenterology and Metabology, Ehime University Graduate School of Medicine, Ehime, Japan
2 Department of Medical Science, Toshiba General Hospital, Tokyo, Japan

Keywords
hepatic NK cells – immune tolerance – interleukin-10 – liver immunity – regulatory NK cells

Correspondence
Sheikh Mohammad Fazle Akbar, MD, PhD, Department of Medical Sciences, Toshiba General Hospital, 6-3-22 Higashi Oi, Shinagawa, Tokyo 140-8522, Japan
Tel: +81 3 3764 0511
Fax: +81 3 3764 8992
e-mail: sheikh.akbar@po.toshiba.co.jp

Received 29 September 2009
Accepted 28 March 2010

DOI:10.1111/j.1478-3231.2010.02253.x

Abstract

Background: Abundant amounts of natural killer (NK) cells are present in the liver, most of which are endowed with direct cytotoxic and inflammatory cytokine production capacities. However, the control of compromised immunity in the liver may be accomplished by a population of regulatory NK cells possessing suppressive or tolerogenic functions. *Aims:* To identify and characterize regulatory NK cells in murine liver. *Methods:* NK cells were isolated from the liver of C57BL/6 mice by magnetic-activated cells sorting (MACS). NK cells were stimulated with different agents and those cells that produced interleukin (IL)-10 were detected by flow cytometry and isolated by MACS. IL-10-producing NK cells were regarded as regulatory NK cells and the functional capacities of liver-derived regulatory NK cells were assessed *in vitro*. *Results:* The frequencies of regulatory NK cells in the liver were $4.1 \pm 0.3\%$ of hepatic NK cells and $0.45 \pm 0.02\%$ of liver nonparenchymal cells. Regulatory NK cells produced abundant amounts of IL-10 in culture. These cells also suppressed the proliferative capacities of T cells and B cells *in vitro*. However, another population of NK cells that did not produce IL-10 (immunogenic NK cells) could not suppress lymphocyte proliferation. *Conclusions:* The presence of regulatory NK cells in the liver and their immunosuppressive capacities endowed these cells with the critical function of maintaining homeostasis under normal conditions. Exaggerated or impaired functions of these cells may also contribute to different pathological processes.

Hepatic immunity is a complex and poorly defined area because the exact mechanisms that regulate immunological events of the liver in health and diseases are poorly understood. The liver is composed of hepatic parenchyma cells (nearly 70% of total cellular population), liver nonparenchymal cells (NPCs, nearly 30%) and intracellular matrix (1). The liver remains at the centre of immune tolerance and immune responses. Different food products, inflammatory substances, allergens and drug metabolites constantly enter the liver through the gut or the bloodstream. Under physiological conditions, the liver induces a state of immunological tolerance to these substances to prevent extreme and detrimental immune reactions (2). On the other hand, many hepatotrophic viruses including hepatitis A to E viruses, parasites and bacteria enter the liver and induce antimicrobial immunity, which ultimately leads to the inflammation and destruction of hepatocytes (3, 4). Taken together, hepatic homeostasis is maintained by a highly regulated and well-coordinated balance between the tolerogenic and immunogenic properties of different immunocytes.

Studies have revealed that most of the immunocytes are capable of inducing both tolerance and immunity. Macrophages are well known for their phagocytic activities and production of abundant amounts of inflammatory cytokines, but some specific cells of their lineage have tolerogenic capacities (5, 6). Dendritic cells (DC) are initiators and regulators of immune responses because they can recognize, process, and present antigens to lymphocytes for the induction of immunity (7). However, regulatory DC downregulate the magnitude of immunity and thus play an important role in the maintenance of homeostasis (8). Similarly, immunogenic T cells and regulatory T cells ensure balanced immunity (9).

In this context, natural killer (NK) cells have occupied an interesting and puzzling position in hepatic immunity (10–12). They are regarded as basic pillars of innate immunity by virtue of their potent capacities to contain microbial agents, viral-infected cells and cancer cells. These functions are mediated by their direct cell-killing properties (cytotoxic NK cells) or by the production of inflammatory cytokines (immunogenic NK cells).

However, how compromised innate immunity can be regulated in the presence of only one population of cytotoxic or immunogenic NK cells remains unknown. The issue becomes more important because the frequency of NK cells is usually higher in the liver compared with those in other parenchymal organs (13). In this context, the existence of immunosuppressive NK cells that produce interleukin (IL)-10, an anti-inflammatory cytokine, has been reported in murine decidua and human peripheral blood (14, 15). However, it remains unclear whether immunosuppressive or immunoregulatory NK cells are present in the liver.

This study was performed to detect immunoregulatory NK cells in the liver by looking for a population of IL-10-producing NK cells in murine liver. A trace population of hepatic NK cells produced IL-10 in culture. We isolated IL-10-producing regulatory NK cells and assessed their functional capacities *in vitro*.

Materials and methods

Mice

Adult male C57BL/6J (H-2K^b) mice were purchased from Nihon Clea (Tokyo, Japan). The mice were housed in polycarbonate cages in a temperature-controlled room (23 ± 1 °C) with a 12-h light/dark cycle in the pathogen-free animal housing facility at Ehime University Graduate School of Medicine. All animals received humane care and study protocols were in compliance with the institution's guidelines.

Isolation of T lymphocytes and B lymphocytes from the spleen and the liver

We have previously described in detail the methodologies for isolating spleen cells and liver NPCs (16, 17). To produce a single cell suspension from the spleen, the spleens were cut into pieces and passed through a 40-μm pore-size nylon filter (BD Falcon, Durham, NC, USA); the resulting cells were collected and suspended in a culture medium [RPMI 1640 (Iwaki, Osaka, Japan) plus 10% fetal calf serum (Filtron PTY Ltd., Brooklyn, Australia)].

To retrieve liver NPCs, liver tissues were cut into pieces, homogenized, passed through 70-μm pore-size steel meshes (Morimoto Yakuhin Co., Matsuyama, Japan) and suspended in 35% percoll (Sigma Chemical, St Louis, MO, USA). After centrifugation for 15 min at 450*g* at room temperature, a high-density cell pellet was collected and suspended in a culture medium.

T lymphocytes and B lymphocytes were isolated from a spleen single-cell suspension and liver NPCs by a negative selection column method using a mouse pan T isolation kit and a mouse pan B isolation kit (Miltenyi Biotec, Bergish Gladbach, Germany) according to the directions of the manufacturer (18).

Isolation of natural killer cells

Spleen NK cells and liver NK cells were isolated from single-cell suspensions of the spleen and liver NPCs, respectively, by a negative cell selection method using an NK isolation kit (Miltenyi Biotec) with a magnetic-activated cell sorting (MACS) system (AutoMACS, Miltenyi Biotec).

Estimation of interleukin-10- and interferon-γ-producing natural killer cells by the cytometric bead array method

Freshly isolated NK cells were stimulated with CpG oligodeoxynucleotide (CpG ODN; 1 μg/ml, Invitrogen, San Diego, CA, USA), concanavalin A (Con A, 1 μg/ml, Sigma), lipopolysaccharides (LPS, 1 μg/ml, Sigma), CL-097 (1 μg/ml, Invitrogen) and herpes simplex virus-1 (HSV-1, 1×10^5 plaque-forming units, kindly provided by Prof. Masaki Yasukawa, Department of Bioregulatory Medicine, Ehime University Graduate School of Medicine, Ehime, Japan) for 72 h. The levels of IL-10 and interferon (IFN)-γ in culture supernatants were estimated using a commercial kit for the cytometric bead array method, as described previously (18). The levels of IL-10 and IFN-γ in the culture supernatants were calibrated from the mean fluorescence intensities of the standard negative control, standard positive control and samples by cytometric bead array software (BD Biosciences Pharmingen, San Jose, CA, USA) using a Macintosh computer (SAS Institute, Cary, NC, USA). The amounts of IL-10 and IFN-γ were expressed as pg/ml.

Flow cytometric detection of regulatory natural killer cells

Because we found that CpG ODN was the most potent stimulator of IL-10 in NK cells, CpG ODN was used in subsequent experiments to detect regulatory NK cells. The detection of IL-10-producing NK cells was performed according to a method described previously (19). We stimulated freshly isolated NK cells with CpG ODN (1 μg/ml) overnight. After stimulation, cells were labelled with anti-IL-10/CD45 antibody–antibody conjugates (Miltenyi Biotec) for 10 min. After washing, cells were resuspended in 37 °C medium to secrete IL-10 for 45 min. Subsequently, cells were washed and stained with phycoerythrin (PE)-conjugated anti-IL-10 for 10 min. After washing with a washing buffer, cells were incubated with FITC-conjugated anti-NK1.1 (BD Biosciences Pharmingen) and PE-conjugated anti-IL-10. Next, IL-10-secreting NK cells were detected by two-colour flow cytometry.

Isolation of interleukin-10-producing regulatory and immunogenic natural killer cells by magnetic-activated cell sorting

We stimulated NK cells with CpG ODN for their detection by flow cytometry as well as for the isolation of

regulatory NK cells. After detecting IL-10-producing NK cells with PE-conjugated anti-IL-10, we additionally labelled the cells with anti-PE microbeads, as described previously (19). The IL-10-producing NK cells (regulatory NK cells) were isolated by a positive selection method using MACS (15). The cells of negative fraction, non-IL-10 producing cells, were regarded as immunogenic NK cells. These cells were suspended in RPMI 1640 medium plus 10% fetal calf serum.

Enzyme-linked immunospot assay

Freshly isolated 1×10^5 NK cells were stimulated with CpG ODN in an IL-10-coated enzyme-linked immunospot (ELISPOT) plate (Mabtech, Nacka Strand, Sweden) for 24 h. After the cells were removed, a detection antibody (2A5-biotin) was added to the wells. After 2 h of incubation, the plates were incubated with streptavidin–alkaline phosphatase for 1 h. After the plate was washed, the substrate solution, BCIP/NBT, was put into each well. The reaction was stopped by washing the plates extensively with tap water. The numbers of spot-forming units (SFU) were counted using an ELISPOT reader (KS ELISPOT, Carl Zeiss, Thornwood, NY, USA) and were deducted from number of background SFU of control wells. The data were finally shown as numbers of SFU/well.

Lymphoproliferative assays

T cells and B cells (1×10^5 cells/200 μl well) were stimulated with Con A and LPS in a U-bottom 96-well plate (Corning, Tokyo, Japan) with or without regulatory NK cells and immunogenic NK cells for 120 h. [^{3}H]-thymidine (1.0 μCi/ml, Amersham Biosciences UK Ltd., Little Chalfont, Buckinghamshire, UK) was diluted in sterile RPMI 1640 medium and added to the cultures for the last 16 h. The cells were harvested automatically by a multiple cell harvester (LABO MASH, Futaba Medical, Tokyo, Japan) onto filter paper (LM 101-10, Futaba Medical). The levels of incorporation of [^{3}H]-thymidine (1.0 mCi/L, Amersham Biosciences UK Ltd., Little Chalfont, Buckinghamshire, UK) were determined in a liquid scintillation counter (Beckman-LS 5000, Beckman Instruments Inc., Fullerton, CA, USA) from the level of blastogenesis. The levels of blastogenesis in cultures without regulatory NK cells or immunogenic NK cells were regarded as the control. The data were expressed as counts per minute (CPM).

Statistical analysis

Data were analysed by unpaired *t*-tests if the data were normally distributed and by the Mann–Whitney rank-sum test if they were skewed. Data were expressed as means ± standard error of mean (mean ± SEM). Differences were considered significant if $P<0.05$.

Results

Interleukin-10 production by natural killer cells in response to stimulation by CpG oligodeoxynucleotide

We checked the capacity of IL-10 production of freshly isolated NK cells from the liver because of stimulation with various stimulants, as described in the 'Methods' section. The production of IL-10 by liver NK cells was stimulated with all stimulants; however, stimulation with CpG ODN induced the maximum amounts of IL-10 (Fig. 1a). Conversely, CpG ODN induced relatively lower amounts of IFN-γ compared with other stimulants (Fig. 1). Accordingly, CpG ODN was used to induce IL-10 in successive experiments to detect regulatory NK cells.

Detection of interleukin-10-producing natural killer cells by enzyme-linked immunospot

We obtained evidence that NK cells produced considerable amounts of IL-10 because of stimulation with CpG ODN. To obtain further evidence of IL-10 production by NK cells, we performed an IL-10-specific ELISPOT assay. As shown in Fig. 2, NK cells stimulated with CpG ODN produced IL-10-specific spots in the ELISPOT assay; however, almost no spot was detected in unstimulated NK cells. The SFU value in the control culture without stimulation was $3.0 \pm 1.0/1 \times 10^5$cells. On the other hand, the SFU value was $163.7 \pm 7.1/1 \times 10^5$ cells ($P < 0.01$) in cultures containing CpG ODN-stimulated NK cells.

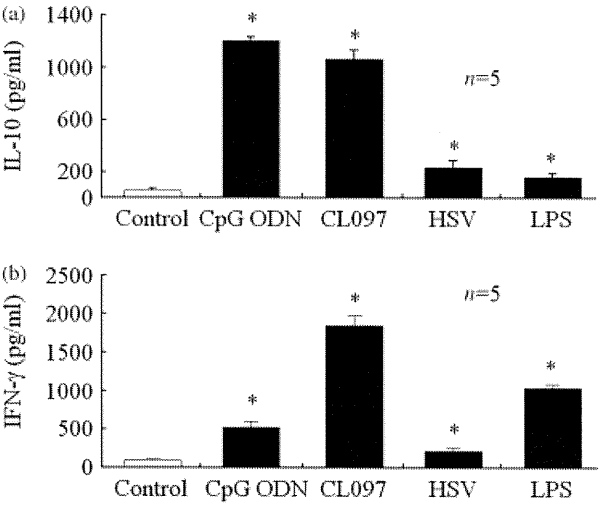

Fig. 1. Induction of interleukin (IL)-10 from liver natural killer (NK) cells. Liver-derived NK cells were stimulated with CpG ODN (CpG oligodeoxynucleotide, a double-stranded DNA), CL097 (an agonist of toll-like receptor 8), herpes simplex virus-1 (HSV-1), and lipopolysaccharide (LPS) for 24 h. The amounts of IL-10 (a) and interferon (IFN)-γ (b) in culture supernatant were measured by the cytometric bead array method and expressed as pg/ml. The mean and SEM of five separate experiments are shown. *$P < 0.05$, compared with control (not stimulated with any stimulant).

Increased frequency of regulatory natural killer cells in the liver

A representative staining pattern of NK cells and IL-10-producing regulatory NK cells in the spleen and the liver is shown in Fig. 3. First, we estimated the frequency of NK cells in the spleen and the liver [cells in the upper left quadrant ($NK1.1^+$ and $CD3^-$)] (Fig. 3a). The amounts of NK cells in the liver were about three times of those in the spleen. Next, we stimulated freshly isolated NK cells with CpG ODN to induce IL-10 production. Subsequently, regulatory NK cells that produced IL-10 were detected by flow cytometry and their frequencies were assessed. The frequency of IL-10-producing NK cells was almost similar in the liver and the spleen (Fig. 3b). However, the frequencies of total NK cells were significantly higher in the liver (Fig. 3a). Accordingly, the ultimate proportion of regulatory NK cells was significantly higher in the liver ($0.45 \pm 0.02\%$, $n = 5$) than in the spleen ($0.15 \pm 0.03\%$, $n = 5$) ($P < 0.05$) (Table 1).

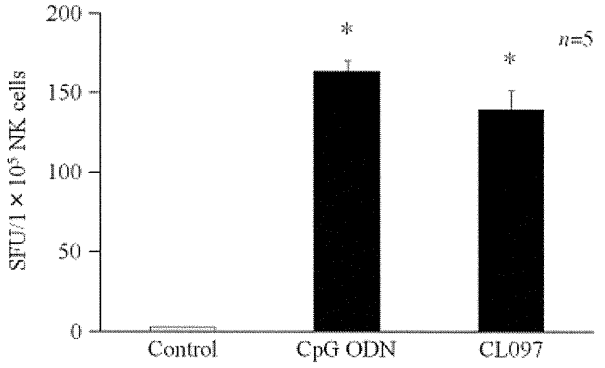

Fig. 2. Interleukin (IL)-10 production by liver natural killer (NK) cells in an enzyme-linked immunospot (ELISPOT) assay. Liver-derived NK cells isolated by a magnetic cell sorter were checked for IL-10 production in an ELISPOT assay after stimulation with CpG oligodeoxynucleotide (CpG ODN) and CL-097. Almost no IL-10 was produced by NK cells without activation by stimulators (Control). Abundant numbers of IL-10-specific spots because of stimulation with CpG ODN and CL-097. Data of five separate experiments have been shown. $^*P < 0.05$, compared with controls.

Suppressive effects of regulatory natural killer cells on T cells proliferation

To assess the functional capacities of regulatory NK cells, the effect of these cells on mitogen-induced lymphocyte proliferation was evaluated. T cells and B cells were stimulated with Con A and LPS, respectively, without or in the presence of regulatory NK cells. The levels of blastogenesis of T cells (1×10^5 cells) owing to stimulation with Con A were $77\,502 \pm 13\,407$ CPM ($n = 5$).

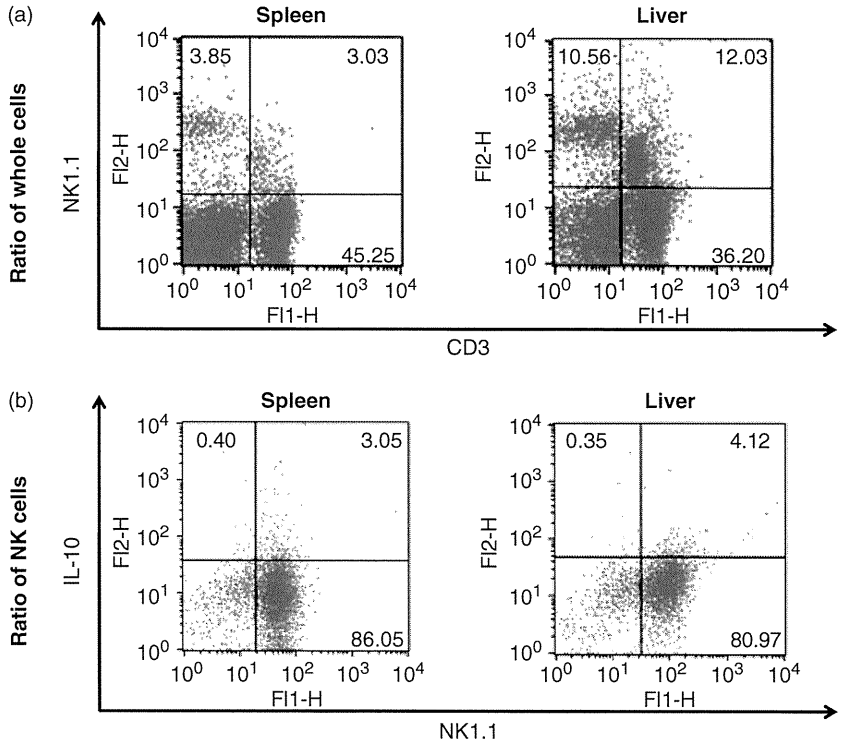

Fig. 3. Flow cytometric detection of natural killer (NK) cells and regulatory NK cells in the spleen and the liver. A representative staining pattern of NK cells and interleukin (IL-10)-producing regulatory NK cells have been shown. (a) Natural killer cells were defined by $NK1.1^+$ and $CD3^-$ fraction by dual-colour flow cytometry. The cells in the upper left quadrant indicate NK cells. (b) NK cells were isolated from the spleen and the liver. NK cells were stimulated with CpG oligodeoxynucleotide and regulatory NK cells were confirmed by expressions of IL-10, as described in the Methods section. Cells in the right upper quadrant are IL-10-producing regulatory NK cells.

However, the addition of 1×10^4 IL-10-producing regulatory NK cells caused a significant reduction of levels of blastogenesis (56 326 ± 3286 CPM ($n = 5$, $P < 0.05$) (Fig. 4). Similarly, the levels of LPS-induced proliferation of B cells (1×10^5 cells) were 34 950 ± 599 CPM ($n = 5$). The addition of regulatory NK cells (1×10^4 cells) caused a significant suppression of levels of B cells proliferation (25 073 ± 971 CPM) ($n = 5$) ($P < 0.05$) (Fig. 4).

Immunogenic effect of nonregulatory natural killer cells

To develop more insights on the role of NK cells and regulatory NK cells in T and B cells proliferation, we isolated a population of NK cells that did not produce IL-10. These cells were regarded as immunogenic NK cells. As expected, the immunogenic NK cells induced an increased proliferation of T cells in the presence of Con A (levels of blastogenesis; without immunogenic NK cells vs with immunogenic NK cells, 60 179 ± 3642 CPM vs 85 475 ± 4753 CPM, $n = 5$, $P < 0.05$) (Fig. 5). Similarly, immunogenic NK cells induced a significantly higher proliferation of B cells in the presence of LPS ($P < 0.05$) (Fig. 5).

Table 1. Frequencies of different immunocytes in spleen cells and liver nonparenchymal cells

	Liver	Spleen
T cells	34.6 ± 1.6	40.5 ± 3.3
B cells	32.2 ± 1.5	47.1 ± 1.2
Natural killer (NK) cells	11.0 ± 0.5*	4.6 ± 0.4
Regulatory NK cells	0.45 ± 0.02*	0.15 ± 0.03
Natural killer T cells	14.6 ± 1.2	3.9 ± 0.5
Monocytes	12.6 ± 2.3	8.6 ± 1.9

Different populations of immunocytes among single cell suspensions from the spleen and nonparanchymal cells of the liver were assessed by flow cytometry. Data of five separate experiments are shown.
*$P < 0.05$, compared with that of spleen.

Discussion

Natural killer cells represent a primary pillar of innate immunity and are endowed with excellent capacities to destroy different types of cells. They also produce various proinflammatory cytokines. It is natural to assume that NK cells ensure an inflammatory mucosal milieu *in vivo*. However, an exception to this rule is observed in the context of hepatic immunity. The liver harbours increased frequencies of NK cells compared with other parenchymal organs (13). However, the liver is recognized as a tolerogenic organ because most of the dangerous and nonself elements entering the liver do not induce immune responses (20). Moreover, the liver is comparatively resistant to transplant rejection even in the context of HLA mismatch transplantation (21). These realities suggest that some immunocytes of the liver may have a potent tolerogenic activity; however, the nature of these cells has not been properly explored until now.

We targeted NK cells to determine the role of these cells in hepatic tolerance because tolerogenic NK cells have been detected in placental decidua and peripheral blood and they have been referred to as regulatory NK cells (14, 15).

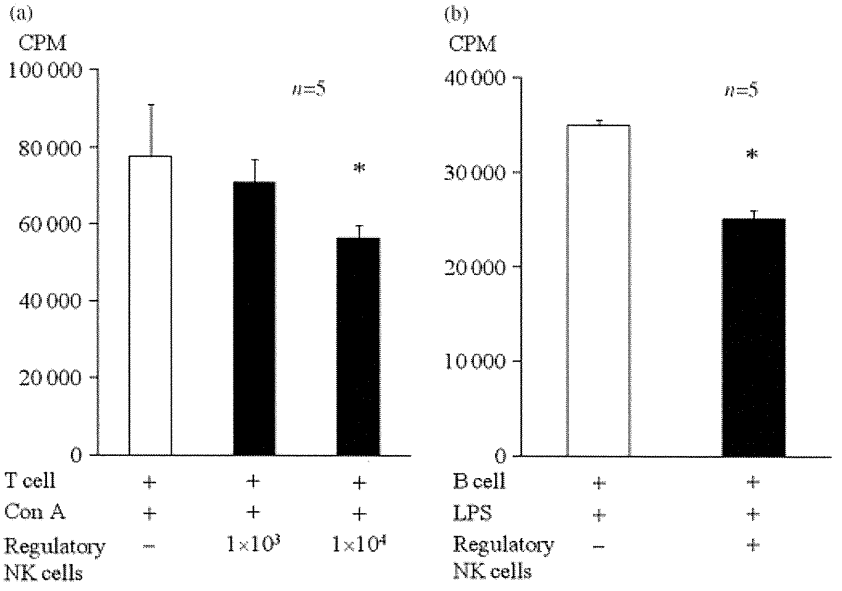

Fig. 4. Suppression of the proliferation of lymphocytes by liver regulatory natural killer (NK) cells. T cells and B cells were stimulated by concanavalin A (Con A) (a) and lipopolysaccharides (LPS) (b), and with or without regulatory NK cells. The levels of proliferation of T cells and B cells were shown as counts per minute (CPM). Data are shown as mean and standard error of mean of five separate experiments. The addition of hepatic regulatory NK cells suppressed the proliferation of T and B cells. Data of five separate experiments have been shown. *$P < 0.05$, compared with proliferation of T and B cells in the absence of regulatory NK cells.

Liver International (2010)

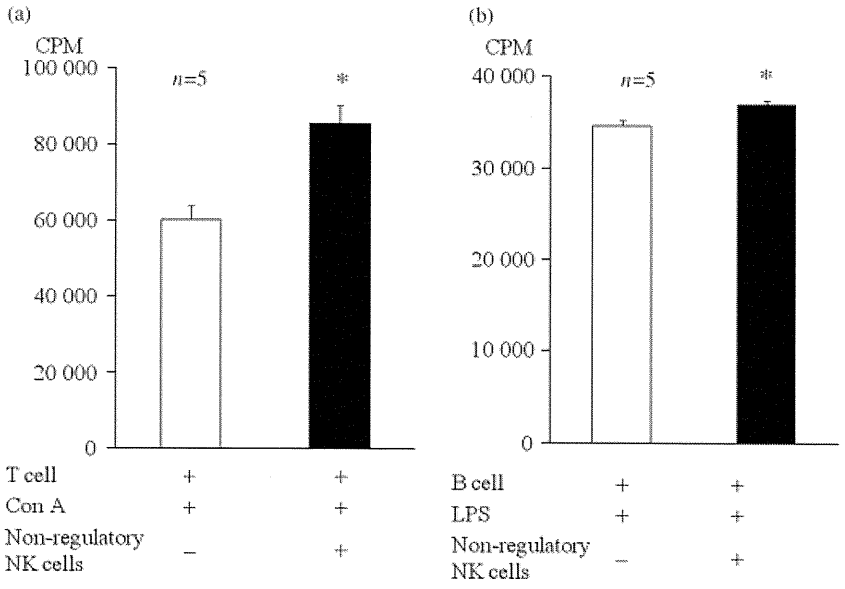

Fig. 5. Accentuation of T cell and B cells proliferation by non-IL-10-producing hepatic natural killer (NK) cells. T cells and B cells were cultured with concanavalin A (Con A) (a), lipopolysaccharides (LPS) (b), and with or without non-IL-10-producing NK cells (immunogenic NK cells). Increased T cell and B cell proliferation was observed due to the addition of non-IL-10-producing NK cells. Data of five separate experiments have been shown. $^*P < 0.05$, compared with controls.

Natural killer cells have many kinds of receptors including immunoglobulin-like receptors lectin-like receptors. NK cells also express toll-like receptors, TLR-2, TLR-3, TLR-4, TLR-7, TLR-8 and TLR-9 (22). To prepare regulatory NK cells, we took the advantage of the expression of TLR-9 on NK cells. In this study, we have shown that a population of NK cells in the liver produced abundant amounts of IL-10 in response to stimulation with CpG ODN. In fact, most of the immune activators induced IL-10 from liver NK cells; however, CpG ODN was the most potent stimulant. Interestingly, CpG ODN induced very low levels of IFN-γ from NK cells in this study. Our observations might come from the tolerogenic aspect of CpG ODN. CpG ODN is known to induce IL-10 production from B cell and macrophage and is now used for the treatment of allergy and asthma (23).

The frequencies of regulatory NK cells were significantly higher in the liver compared with those in the spleen. Functionally, regulatory NK cells of the liver had immunosuppressive properties in the context of mitogen-induced T and B cell proliferation.

Most of the NPCs of the liver, such as DCs, liver sinusoidal endothelial cells, Kupffer cells, hepatic stellate cells, and regulatory T cells are responsible for the tolerogenic properties of the liver (24, 25). One of the important factors that endow tolerogenic property of these cells is their capacity to produce significant amounts of IL-10. This study has shown that regulatory NK cells represent another NPC, capable of producing abundant amounts of IL-10. We have also shown another population of IFN-γ-producing NK cells in the liver. Several immunocytes have shown both immunogenic and tolerogenic potentials; (i) immunogenic DCs and regulatory DCs and (2) effecter T cells and regulatory T cells. Further study will be required to assess whether regulatory NK cells regulate the functional capacities of immunogenic NK cells or whether they are endowed with wide variety of immune suppressive functions.

This is the first study that showed the presence and functional features of regulatory NK cells in healthy murine liver. However, many aspects of this unique population of NK cells could not be properly addressed by our study. We had to stimulate liver NK cells with an immunostimulator to obtain IL-10-producing regulatory NK cells. This raises a question about the presence of these cells *in vivo* in pathogen-free conditions in the healthy liver. Decidual NK cells are thought to migrate from peripheral blood and differentiate into decidual NK cells; they then obtain their regulatory function because of the decidua's tolerogenic microenvironment (26). Liver is also considered to be a tolerogenic organ and it is possible that peripheral NK cells differentiate into regulatory NK cells and obtain immunosuppressive functions in the liver microenvironment.

In addition to their role in maintaining homeostasis, regulatory NK cells may also play a role in the pathogenesis of different liver-related diseases. Inadequate immune responses are detected in patients with chronic hepatitis B virus and hepatitis C virus (HCV) infections. On the other hand, distorted immune responses are seen in subjects with autoimmune liver diseases. Patients infected with HCV had more IL-10-producing NK cells compared with healthy controls and IL-10-producing regulatory NK cells might be involved in HCV persistence (27). Also, NK cells are suspected to be related with

autoimmunity and autoimmune diseases. Disruption of the critical balance between immunogenic NK cells and regulatory NK cells may regulate the autoimmune process of the liver. However, further studies about regulatory NK cells are likely to answer some queries regarding these conditions.

In conclusion, this study has shown that regulatory NK cells are present in the liver, just as their existence has been reported in placenta and peripheral blood. Also, their possible immunosuppressive role has been elucidated by this study. Further study will unveil the real implications of these cells in physiological and pathological conditions.

Acknowledgements

We would like to thank the Integrated Centre for Science, Shigenobu Station, Ehime University for animal management. This study was supported in part by a grant from Miyakawa Memorial Research Foundation, Tokyo, Japan to Dr S. M. F. Akbar and a grant-in-aid from the Ministry of Health Welfare, Japan to Dr M. Abe.

References

1. Mehal WZ, Azzaroli F, Crispe IN. Immunology of the healthy liver: old questions and new insights. *Gastroenterology* 2001; **120**: 250–60.
2. Crispe IN, Dao T, Klugewitz K, Mehal WZ, Metz DP. The liver as a site of T-cell apoptosis: graveyard or killing field? *Immunol Rev* 2000; **174**: 47–62.
3. Das A, Hoare M, Davies N, *et al.* Functional skewing of the global CD8 T cell population in chronic hepatitis B infection. *J Exp Med* 2008; **205**: 2111–24.
4. Bowen DG, Walker CM. Adaptive immune responses in acute and chronic hepatitis C infection. *Nature* 2005; **436**: 946–52.
5. Crofton RW, Disselhoff-den Dulk MM, van Furth R. The origin, kinetics, and characteristics of the Kuppffer cells in the normal steady state. *J Exp Med* 1978; **148**: 1–17.
6. Knolle P, Schlaak J, Uhring A, *et al.* Human Kuppffer cells secrete IL-10 in response to lipopolysaccharides (LPS) challenge. *J Hepatol* 1995; **22**: 226–9.
7. Akbar SM, Abe M, Yoshida O, Murakami H, Onji M. Dendritic cell-based therapy as a multidisciplinary approach to cancer treatment: present limitations and future scopes. *Curr Med Chem* 2006; **13**: 3113–9.
8. Steinman RM, Nussenzweig MC. Avoiding horror autotoxicus: the importance of dendritic cells in peripheral T cell tolerance. *Proc Natl Acad Sci USA* 2002; **99**: 351–8.
9. Sakaguchi S, Sakaguchi N, Asano M, Itoh M, Toda M. Immunogenic self-tolerance maintained by activated T cell expressing IL-2 receptor α-chains (CD25). *J Immunol* 1995; **115**: 1151–64.
10. Notas G, Kisseleva T, Brenner D. NK and NKT in liver injury and fibrosis. *Clin Immunol* 2009; **130**: 16–26.
11. Yamagiwa S, Kamimura H, Ichida T. Natural killer receptor and their ligands in liver diseases. *Med Mol Morphol* 2009; **42**: 1–8.
12. Jeong WI, Park O, Radaeva S, Gao B. STAT1 inhibits liver fibrosis in mice by inhibiting stellate cell proliferation and stimulating NK cell cytotoxicity. *Hepatology* 2006; **44**: 1441–51.
13. Racanelli V, Rehermann B. The liver as an immunological organ. *Hepatology* 2006; **43**: S54–62.
14. Saito S, Nakashima A, Myojo-Higma S, Shiozaki A. The balance between cytotoxic NK cells and regulatory NK cells in human pregnancy. *J Reported Immunol* 2008; **77**: 14–22.
15. Deniz G, Erten G, Kucuksezer UC, *et al.* Regulatory NK cells suppress antigen-specific T cell responses. *J Immunol* 2008; **15**: 850–7.
16. Akbar SM, Onji M, Inaba K, Yamamura K-I, Ohta Y. Low responsiveness of hepatitis B virus transgenic mice in antibody response to T-cell-dependent antigen. *Immunology* 1993; **87**: 468–73.
17. Hasebe A, Akbar SM, Furukawa S, Horiike N, Onji M. Impaired functional capacities of liver dendritic cells from murine hepatitis B virus (HBV) carriers. *Clin Exp Immunol* 2005; **139**: 35–42.
18. Yoshida O, Akbar F, Miyake T, *et al.* Impaired dendritic cell functions because of depletion of natural killer cells disrupt antigen-specific immune responses in mice. *Clin Exp Immunol* 2008; **152**: 174–81.
19. McAllister F, Steele C, Zheng M, *et al.* T cytotoxic-1 CD8+T cells are effecter cells against pneumocystis in mice. *J Immunol* 2004; **172**: 1132–8.
20. Crispe IN. The liver as a lymphoid organ. *Annu Rev Immunol* 2009; **27**: 147–63.
21. Knechtle SJ, Kalayolu M, D'Alessandro AM, *et al.* Histocompatibility and liver transplantation. *Surgery* 2003; **114**: 667–71.
22. O'Connor GM, Hart OM, Gardiner CM. Putting the natural killer cell in its place. *Immunology* 2006; **117**: 1–10.
23. Verthelyi D, Klinman DM. Immunoregulatory activity of CpG oligonucleotides in humans and nonhuman primates. *Clin Immunol* 2003; **109**: 64–71.
24. Tiegs G, Lohse AW. Immune tolerance: what is unique about the liver. *J Autoimmun* 2010; **34**: 1–6.
25. Knolle PA, Gerken G. Local control of the immune responses in the liver. *Immunol Rev* 2000; **174**: 21–34.
26. Santoni A, Zingoni A, Cerboni C, Gismondi A. Natural killer (NK) cells from killer to regulator: distinct features between peripheral blood and decidual NK cells. *Am J Reprod Immunol* 2007; **58**: 280–8.
27. De Maria A, Fogli M, Mazza S, *et al.* Increased natural cytotoxity receptor expression and relevant Il-10 production in NK cells from chronically infected viremic HCV patients. *Eur J Immunol* 2007; **37**: 445–55.

Virtual Puncture Line in Radiofrequency Ablation for Hepatocellular Carcinoma of the Caudate Lobe

Masashi Hirooka[1]
Yoshiyasu Kisaka
Kazuhiro Uesugi
Yohei Koizumi
Masanori Abe
Yoichi Hiasa
Morikazu Onji

OBJECTIVE. In this study, we evaluated the feasibility of using a virtual puncture line in 3D CT for the treatment of 21 hepatocellular carcinoma (HCC) nodules in the caudate lobe.

CONCLUSION. There were no severe complications in this study. Thus, the treatment of HCC nodules in the caudate lobe using a virtual puncture line is feasible.

Hepatocellular carcinoma (HCC) arising in the caudate lobe of the liver is not usual. The caudate lobe is located deep between the hepatic hilum and inferior vena cava. Percutaneous local ablation therapy is risky. Thus, treatment of HCC in the caudate lobe is limited because of the difficulty in accessing the lesion safely. It is important to select the puncture route using imaging guidance with various techniques, such as CT, CT arterial portography, or CT hepatic arteriography. In this study, we evaluated the feasibility and safety of using a virtual puncture line in 3D CT for the treatment of HCC in the caudate lobe.

Technique

Virtual Puncture Line

For synthesis of 3D images and generation of virtual ultrasound images, Virtual Place Advance software (AZE) was used. First, a 3D image was synthesized by CT (LightSpeed Ultra 16, GE Healthcare). The scanning parameters were 0.625-mm collimation × 16; pitch, 1.75; table speed, 300–400 mA; 120 kV; and 512 × 512 matrix. After imaging, a virtual sonogram of the CT image was generated. Virtual sonography was reshaping the CT image to a convex probe-like image on ultrasound. The dotted line showing the planned puncture line was shown on the virtual sonogram (Fig. 1C). This virtual puncture line was reflected on other 3D images synthesized by CT (Fig. 1D). This 3D image including the virtual image can be viewed from any angle, and the anatomic structure can be analyzed in detail.

Radiofrequency Ablation

Before treatment, 15 mg of pentazocine hydrochloride and 25 mg of hydroxyzine hydrochloride were administered intramuscularly. Local anesthesia was induced by 5 mL of 1% lidocaine injected through the skin into the peritoneum along a predetermined puncture line. We inserted a 20-cm-long, 17-gauge radiofrequency electrode equipped with a 2-cm-long exposed metallic tip (Cooltip, Valleylab). First, abdominal CT was performed and a virtual sonogram of the CT was prepared using the CT data. The most moderate image from the virtual ultrasound that was not deemed to be of important vessels or organs was determined by examining the various oblique axes. The virtual puncture line was made on the virtual sonogram. We confirmed carefully the presence of important vessels and organs through the virtual puncture line on the 3D CT image. The identical conventional ultrasound image for virtual ultrasound was depicted and a radiofrequency ablation needle was inserted. Just before inserting the needle, we confirmed the location of the gastric artery on the conventional ultrasound image to ensure that the treatment would be safe (Fig. 1). If the nodule was not visualized clearly because of obstruction by the lung, 500 mL of saline was injected into the right pleural cavity. If the nodule existed close to the major vessels, ethanol was injected using the same technique.

Estimation of Therapeutic Effect

Dynamic CT was performed 3–5 days after treatment. The necrotic area of the HCC nodule and surrounding liver parenchyma

Keywords: caudate lobe, hepatocellular carcinoma, radiofrequency ablation, virtual puncture line

DOI:10.2214/AJR.08.1817

Received September 11, 2008; accepted after revision February 2, 2009.

[1]All authors: Department of Gastroenterology and Metabiology, Ehime University Graduate School of Medicine, Shizukawa 454, Toon-shi, Ehime 791-0295, Japan. Address correspondence to M. Hirooka (masashih@m.ehime-u.ac.jp).

WEB
This is a Web exclusive article.

AJR 2009; 193:W149–W151

0361–803X/09/1932–W149

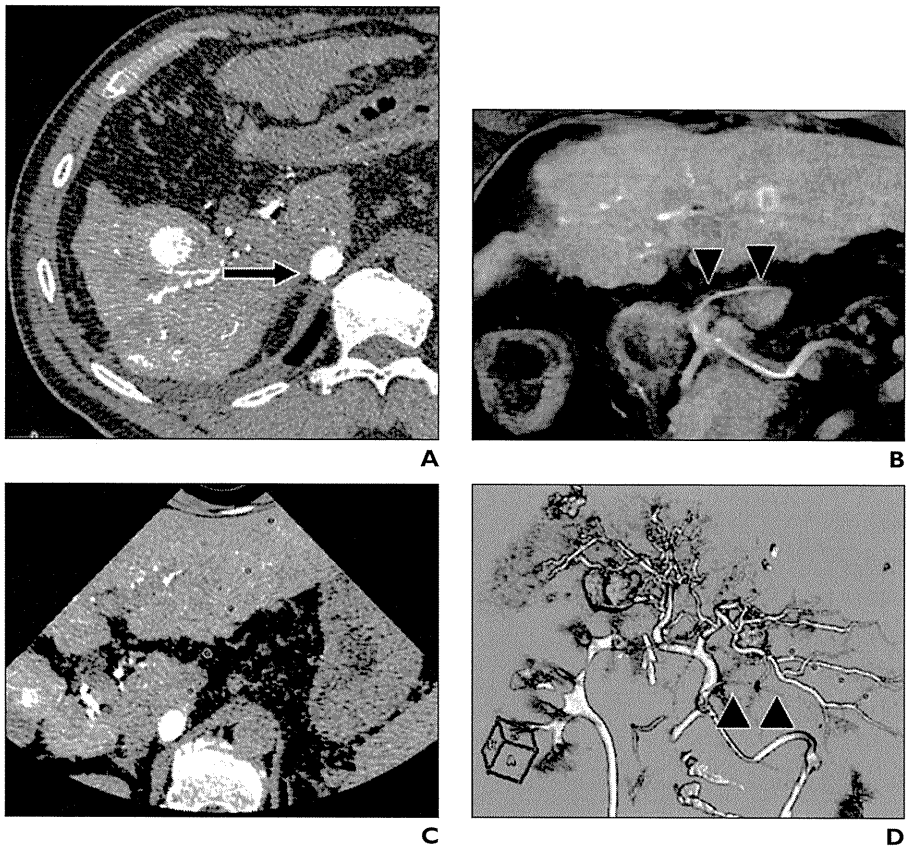

Fig. 1—Creation of virtual puncture line in 56-year-old man with hepatocellular carcinoma arising in Spiegel lobe (case 1).
A, CT during hepatic arteriography shows targeted tumor (*arrow*) in Spiegel lobe.
B, Coronal CT image shows right gastric artery (*arrowheads*) in front of Spiegel lobe.
C, Virtual puncture line is shown by red dotted line on virtual sonogram.
D, Virtual puncture line is also indicated on 3D CT image. This puncture line is away from gastric artery (*arrowheads*), and real puncture through virtual puncture line is safe.

was visualized to be hypoattenuating during the late phases of dynamic CT. The session was defined as the treatment time. All treatments were performed using a virtual puncture line. Repeated dynamic CT was performed every 3 months thereafter, and α-fetoprotein and des-γ-carboxy prothrombin assays were performed before treatment, 1 month after treatment, and every month subsequently.

Results

All 21 patients were treated with radiofrequency ablation (Table 1). However, five nodules were treated with a combination of radiofrequency ablation and ethanol injection because the nodule was close to the extrahepatic major vessels. When the right-side approach was performed, artificial pleural effusion was injected for nine nodules. Of the 12 nodules in the anterior approach, 11 were visualized in the gastric artery on 3D CT. One case that could not be visualized in the gastric artery on 3D images also was not shown on conventional ultrasound. This case was treated carefully, and no complications occurred. There was local recurrence in only one case. Although the treatment of the nodule in the caudate lobe is thought to have a high risk, there were no severe complications in this study. Four cases were treated in overlapping zones with several insertions. These cases also were treated using a virtual puncture line.

Discussion

The central location of the caudate lobe and its intimate relationships with critical vascular structures make it difficult to treat a tumor in this lobe. Local ablation therapy for a tumor in the caudate lobe is highly risky, and the technique for introducing the electrode is difficult. By determining the virtual puncture line before the actual puncture, ablation of the tumor in the caudate lobe can be relatively feasible.

According to the classification of Kumon [1], the caudate lobe consists of three anatomic parts: the Spiegel lobe, the paracaval portion, and the caudate process. The anterior transabdominal approach for nodules in the Spiegel lobe or paracaval portion is often selected. In the anterior approach, the electrode penetrates through the left lobe of the liver, goes into extrahepatic tissue, and then is inserted into the nodule in the caudate lobe. There are a few vessels between the left lobe and the Spiegel lobe, such as the portal vein, hepatic artery, and gastric artery [2, 3]. Of course, it is important to avoid injury to these vessels to avoid severe complications.

The virtual puncture line was useful for confirming whether these important vessels existed on the puncture line. The right-sided approach usually will be selected for the treatment of the nodule in the caudate process. However, the right hepatic vein and major branch of the right portal vein may interfere in this right-sided approach. In this approach, the virtual puncture line was also useful to avoid penetrating these vessels.

Yamakado et al. [4] treated these nodules under CT–fluoroscopic guidance. Radiofrequency ablation under CT–fluoroscopic guidance is often a troublesome treatment. Ideally, radiofrequency ablation is completed under sonographic guidance. Thus, it is important to establish the safety of the puncture route on a sonogram. By using virtual ultrasound and 3D CT images to determine a virtual puncture line that is away from major vessels before radiofrequency ablation, we can perform the radiofrequency ablation

TABLE 1: Hepatocellular Carcinoma Nodules in Study

Case No.	Sex	Age (y)	Child-Pugh Classification	Tumor Diameter (mm)	Location	Approach	No. of Sessions	Local Recurrence
1	M	56	B	15	Spiegel lobe	Anterior	1	No
2	M	76	A	31	Paracaval portion	Anterior	1	No
3	M	79	A	25	Paracaval portion	Right	1	No
4	M	63	A	18	Spiegel lobe	Anterior	1	No
5	M	63	A	15	Paracaval portion	Right	1	No
6	M	82	A	20	Caudate process	Right	2	No
7	M	57	B	18	Paracaval portion	Right	2	No
8	M	57	B	14	Spiegel lobe	Anterior	1	Yes
9	M	60	A	12	Spiegel lobe	Anterior	1	No
10	F	75	A	16	Paracaval portion	Right	1	No
11	F	58	B	23	Spiegel lobe	Anterior	1	No
12	M	80	A	20	Spiegel lobe	Anterior	1	No
13	M	80	A	34	Spiegel lobe	Anterior	2	No
14	M	59	B	23	Caudate process	Right	1	No
15	F	61	A	21	Paracaval portion	Right	1	No
16	M	74	A	40	Spiegel lobe	Right	3	No
17	M	71	A	20	Spiegel lobe	Anterior	2	No
18	M	77	A	17	Paracaval portion	Right	2	No
19	M	55	B	31	Spiegel lobe	Anterior	2	No
20	F	75	B	22	Caudate process	Right	1	No
21	M	63	A	12	Spiegel lobe	Anterior	1	No

safely with conventional ultrasound corresponding to the virtual ultrasound images.

Surgical resection is the most curative treatment for HCC nodules. Technically, the operation is difficult and is more commonly done in conjunction with resection of other portions of the liver [5]. Percutaneous local ablation therapy is less invasive. The residual local recurrence rate is high after subsegmental chemoembolization for HCC in the caudate lobe [6]. In this study the local recurrence rate was very low (2.8%).

In conclusion, treatment of HCC nodules in the caudate lobe using a virtual puncture line is feasible.

References

1. Kumon M. Anatomy of the caudate lobe with special reference to portal vein and bile duct [in Japanese]. *Acta Hepatologica Japonoca* 1985; 26:1193–1199
2. Shibata T, Maetani Y, Ametani F, et al. Efficacy of nonsurgical treatments for hepatocellular carcinoma in the caudate lobe. *Cardiovasc Intervent Radiol* 2002; 25:186–192
3. Ishiko T, Beppu T, Sugiyama T, et al. Radiofrequency ablation with hand-assisted laparoscopic surgery for the treatment of hepatocellular carcinoma in the caudate lobe. *Surg Laparosc Endosc Percutan Tech* 2008; 18:272–276
4. Yamakado K, Nakatsuka A, Akeboshi M, et al. Percutaneous radiofrequency ablation for the treatment of liver neoplasms in the caudate lobe left of the vena cava: electrode placement through the left lobe of the liver under CT–fluoroscopic guidance. *Cardiovasc Intervent Radiol* 2005; 28:638–640
5. Tanaka S, Shimada M, Shirabe K, et al. Surgical outcome of patients with hepatocellular carcinoma originating in the caudate lobe. *Am J Surg* 2005; 190:451–455
6. Terayama N, Miyayama Y, Tatsu H, et al. Subsegmental transcatheter arterial embolization for hepatocellular carcinoma in the caudate lobe. *J Vasc Interv Radiol* 1998; 9:501–508

UICC
global cancer control

IJC
International Journal of Cancer

3-Deazaneplanocin A is a promising therapeutic agent for the eradication of tumor-initiating hepatocellular carcinoma cells

Tetsuhiro Chiba[1,2]*, Eiichiro Suzuki[1,2]*, Masamitsu Negishi[2], Atsunori Saraya[2], Satoru Miyagi[2], Takaaki Konuma[2], Satomi Tanaka[2], Motohisa Tada[1], Fumihiko Kanai[1], Fumio Imazeki[1], Atsushi Iwama[2,3] and Osamu Yokosuka[1]

[1] Department of Medicine and Clinical Oncology, Graduate School of Medicine, Chiba University, 1-8-1 Inohana, Chuo-ku, Chiba 260-8670, Japan
[2] Department of Cellular and Molecular Medicine, Graduate School of Medicine, Chiba University, 1-8-1 Inohana, Chuo-ku, Chiba 260-8670, Japan
[3] JST, CREST, Sanbancho, Chiyoda-ku, Tokyo 102-0075, Japan

Recent advances in stem cell biology have identified tumor-initiating cells (TICs) in a variety of cancers including hepatocellular carcinoma (HCC). Polycomb group gene products such as BMI1 and EZH2 have been characterized as general self-renewal regulators in a wide range of normal stem cells and TICs. We previously reported that Ezh2 tightly regulates the self-renewal and differentiation of murine hepatic stem/progenitor cells. However, the role of EZH2 in tumor-initiating HCC cells remains unclear. In this study, we conducted loss-of-function assay of EZH2 using short-hairpin RNA and pharmacological inhibition of EZH2 by an S-adenosylhomocysteine hydrolase inhibitor, 3-deazaneplanocin A (DZNep). Both *EZH2*-knockdown and DZNep treatment impaired cell growth and anchorage-independent sphere formation of HCC cells in culture. Flow cytometric analyses revealed that the two approaches decreased the number of epithelial cell adhesion molecule (EpCAM)$^+$ tumor-initiating cells. Administration of 5-fluorouracil (5-FU) or DZNep suppressed the tumors by implanted HCC cells in non-obese diabetic/severe combined immunodeficient mice. Of note, however, DZNep but not 5-FU predominantly reduced the number of EpCAM$^+$ cells and diminished the self-renewal capability of these cells as judged by sphere formation assays. Our findings reveal that tumor-initiating HCC cells are highly dependent on EZH2 for their tumorigenic activity. Although further analyses of TICs from primary HCC would be necessary, pharmacological interference with EZH2 might be a promising therapeutic approach to targeting tumor-initiating HCC cells.

Cancer Cell Biology

Although first proposed approximately 50 years ago, the concept of cancer stem cells (CSCs) has drawn renewed attention from many oncologists in recent years.[1] According to the concept, tumors consist of a minor component of tumorigenic cells and a major component of non-tumorigenic cells.[2] The minor population, termed CSCs or tumor-initiating cells (TICs), organize a cellular hierarchy in a similar fashion to normal stem cell systems and exhibit pronounced tumorigenic activity in xenograft transplantation.[3,4] Recent progress in stem cell biology and technologies has facilitated the identification of TICs in a variety of cancers.[5] We previously applied side population (SP) analysis and cell sorting to

Key words: hepatocellular carcinoma, cancer stem cell, tumor-initiating cell, EZH2, DZNep

Abbreviations: 5-aza-dC: 5-aza-2′-deoxycytidine; 5-FU: 5-fluorouracil; AFP: α-fetoprotein; ALB: albumin; APC: allophycocyanin; APOC3: apolipoprotein C3; CASP3: active caspase-3; CSC: cancer stem cell; CYP1A2: cytochrome P450: subfamily 1: polypeptode 2; DZNep: 3-deazaneplanocin A; EGFP: enhanced green fluorescent protein; EpCAM: epithelial cell adhesion molecule; H3K27: histone H3 at lysine27; HCC: hepatocellular carcinoma; HMT: histone methyltransferase; Luc: luciferase; MACS: magnetic activated cell sorting; NOD/SCID: non-obese diabetic/severe combined immunodeficient; PcG: polycomb group; PEPCK: phosphoenolpyruvate carboxykinase; PRC: polycomb repressive complex; RT-PCR: reverse transcription-polymerase chain reaction; shRNA: short hairpin RNA; SP: side population; TIC: tumor-initiating cell.

Additional Supporting Information may be found in the online version of this article.

*T.C. and E.S. contributed equally to this work.

Grant sponsors: Global COE Program (Global Center for Education and Research in Immune System Regulation and Treatment), The Ministry of Education, Culture, Sports, Science and Technology, Japan, Core Research for Evolutional Science and Technology (CREST) of Japan Science and Technology Corporation (JST), The Nakayama Cancer Research Institute, The Foundation for the Promotion of Cancer Research

DOI: 10.1002/ijc.26264

History: Received 28 Jan 2011; Accepted 7 Jun 2011; Online 29 Jun 2011

Correspondence to: Atsushi Iwama, Department of Cellular and Molecular Medicine, Graduate School of Medicine, Chiba University, 1-8-1 Inohana, Chuo ward, Chiba 260-8670, Japan, Tel.: +81-43-2262189, Fax: +[81-43-2262191], E-mail: aiwama@faculty.chiba-u.jp; or Osamu Yokosuka, Department of Medicine and Clinical Oncology, Graduate School of Medicine, Chiba University, 1-8-1 Inohana, Chuo ward, Chiba 260-8670, Japan, Tel.: +81-43-2262083, Fax: +[81-43-2262088], E-mail: yokosukao@faculty.chiba-u.jp